

The horizontal far wake behind a heated or cooled body¹

Wilhelm Schneider², Lukáš Bábóř

*Institute of Fluid Mechanics and Heat Transfer, TU Wien, Building BA, Getreidemarkt 9,
1060 Wien, Austria*

Key words

Wake, buoyancy, free shear layer, horizontal flow, self-similar flow, boundary conditions

Abstract

Buoyancy affects the horizontal wake far downstream of a heated or cooled body, especially a horizontal plate, in an indirect manner via the hydrostatic pressure perturbation. Plane (2D) flow at very large Reynolds and Péclet numbers is considered in the present paper. Both laminar and turbulent flows are investigated, with the aim of providing asymptotic solutions that are suitable as outflow boundary conditions for numerical solutions of the equations of continuity, momentum, thermal energy and, in case of turbulent flow, the balance of turbulent kinetic energy. Dimensionless variables are introduced, using the total heat flow from, or towards, the plate as a parameter. It turns out that the buoyancy effects in the momentum equations and in the turbulent kinetic energy balance, respectively, are of the same order of magnitude and can be characterized by a Richardson number.

The asymptotic expansions for large distances from the plate lead to a set of ordinary differential equations for a self-similar flow field. The interaction between the wake and the potential flow is taken into account by applying Bernoulli's equation as a boundary condition to the momentum equation of the wake. As the thermal energy equation as well as the boundary conditions for the temperature perturbation are homogeneous, the solution of the temperature field contains a free coefficient, which is determined from the over-all thermal energy balance.

The results of the analysis are in remarkable contrast to the classical solutions for the wake flow without buoyancy. In particular, driven by the hydrostatic pressure disturbance, the flow does not decay with increasing distance from the plate. Furthermore, the flow is governed by the total heat flow at the plate, whereas the effect of the drag force acting on the plate is negligible.

The set of ordinary differential equations is solved numerically. For laminar flow, two kinds of solutions are found. One of them describes a flow field containing a region of reversed flow. In case of turbulent flow a turbulence model based on the turbulent kinetic energy balance is applied. In addition the limit of very weak buoyancy effects is considered, leading to power laws in terms of the Richardson number.

¹ Dedicated to Prof. Dr.-Ing. Dr.-Ing. E.h. Klaus Gersten on the occasion of his 95th birthday.

² Corresponding author.

E-Mail address: wilhelm.schneider@tuwien.ac.at

1. Introduction

It has been known for many years that the computation of horizontal, or nearly horizontal, mixed convection flows suffers from severe problems with regard to the outflow boundary conditions [1,2]. If reversed flow far downstream can be excluded, the application of conventional outflow boundary conditions may suffice, even if reversed flow regions occur within the computational domain [3]. However, the problem with outflow boundary conditions persists in case of flows that have, or may have, regions of reversed flow far downstream [4,5]. As was already suggested in [2] and further elaborated in [4], a possible remedy is to apply asymptotic solutions as outflow boundary conditions.

The wake far downstream of a submerged body is, of course, a classical problem of fluid mechanics, commonly considered on the basis of boundary-layer theory, cf. [6], pp. 187-190 (laminar flow) and pp. 669-671 (turbulent flow). If the body is heated or cooled, a thermal wake occurs. Provided buoyancy effects are negligible, the temperature field in free flows is analogous to the velocity field, cf. [6], pp. 218-222, 669-671. If, however, buoyancy forces affect the flow, the analysis of the wake becomes more complicated. The special case of the vertical plane wake above a heated or cooled body was studied analytically, numerically and experimentally in [7], where a comprehensive literature survey is also given. In this case, buoyancy gives rise to a force term in the momentum equation for the main flow direction, yet the asymptotic structure of the far wake remains the same as without buoyancy. Clearly, this would also be the case if the wake were not just vertical but arbitrarily inclined with respect to the horizontal plane. In case of a horizontal wake, however, there is no buoyancy-force component acting in main flow direction, and buoyancy affects the flow only indirectly via a perturbation of the hydrostatic pressure. This effect is well-known for both natural and mixed convection flows over semi-infinite horizontal plates, see [6], pp. 281-289 for a survey. It is remarkable that in case of mixed convection flow over horizontal plates the boundary-layer equations exhibit break-downs and non-uniqueness [5,8]. Regarding free flows, it was shown in [9,10] that indirect natural convection at a horizontal plate of finite length may be the source of horizontal jets. As far as the wake downstream of a horizontal plate of finite length is concerned, the question arises whether the far wake is also horizontal. The answer depends on the over-all flow field. For large Reynolds numbers it was found in [11]³ and further elaborated in [12,13]⁴ that a potential flow is induced in order to satisfy the Kutta condition at the trailing edge of the plate and compensate the hydrostatic pressure perturbation across the wake. At the trailing edge, the flow field exhibits a singularity that was investigated for laminar flow in [14,15]. Concerning the far field, it was already observed in [11] that a decay to free-stream conditions at infinity is not possible for an unbounded flow. Thus, a vertical entrance plane (representing, for instance, the outlet of the plate grid of a flow rectifier) at some distance upstream of the horizontal plate was introduced in [11] and a vanishing vertical velocity component at that entrance plane was prescribed. The flow field can also be bounded by horizontal walls of a channel, where the horizontal plate of finite length is placed [12,13]. Obviously, far downstream of the trailing edge the wake, guided by the channel walls, will become horizontal. The same is true for the flow bounded by a vertical entrance plane, as an analysis of the potential flow obtained in [11] shows.

³ An error in the analysis was detected by the present authors. Revised results are given in [4].

⁴ Corrigendum to [12] by author: All subscripts ought to be $2c$ in Eq. (33). The coefficient $4/\sqrt{\pi}$ has to be added in front of the brackets in Eq. (48). $-\tilde{\theta}_{2h}$ rather than $\tilde{\theta}_{2h}$ is plotted in Fig. 5.

Another possibility of prescribing suitable boundary conditions for the induced potential flow is to assume that the flow far upstream of the plate is slightly inclined with respect to the horizontal, cf. [16,17] and the survey given in [18]. In those cases, however, the far wake cannot be expected to be horizontal.

In previous work [11–13] the analysis was simplified on the basis of various assumptions, e.g. large Reynolds numbers, weak buoyancy effects or small Prandtl numbers. It was also tacitly assumed that the classical hierarchy of matched asymptotic expansions is applicable, i.e. that the boundary layer solution, in leading order, is independent of the induced potential-flow solution. However, under certain conditions, an interaction between the vortex sheet that represents the wake and the induced potential flow may be of importance [19]. The interaction effect is characterized by a suitably defined interaction parameter. Remarkably, solutions of the interaction problem could be obtained in [19] only for values of the interaction parameter below a critical value.

In the present analysis we shall try to keep the number of basic assumptions to a minimum. In particular, arbitrary values of the Prandtl number will be allowed, and the assumption of weak buoyancy effects will be dropped. However, in case of turbulent flow, the limit of vanishing buoyancy will be investigated as an interesting special case. To describe the far wake, asymptotic expansions for large distances from the plate (or another body) will be performed, leading to sets of ordinary differential equations for self-similar laminar and turbulent, respectively, flow fields. The interaction between the wake and the potential flow will be taken into account by applying Bernoulli's equation as a boundary condition to the differential equations.

The presentation is arranged as follows. After defining dimensionless quantities and formulating the basic equations in sections 2 to 4, the laminar wake flow is considered in section 5. However, by analogy to the classical laminar wake flow [20], the buoyant horizontal laminar wake flow can be expected to become unstable and undergo the transition to turbulence already at modestly large local Reynolds numbers. Of course, the streamwise pressure gradient induced by buoyancy can have a strong effect on the stability of the laminar wake, cf. [21]. To study the associated stability and transition problem is beyond the scope of the present investigation. But it appears worthwhile to discuss the main properties of the fully turbulent horizontal wake. This will be done in section 6. The last section is devoted to conclusions and a discussion of the main results of the analysis. Finally, Appendices provide additional material that might be of some interest, but has not been seen as essential for the main problem.

2. Dimensionless variables

The plane steady flow in the wake very far from a horizontal plate (or another body of a shape that prevents oscillations of the wake) is considered; see Fig.1. For turbulent flow, ensemble (or time) averaged quantities are denoted by a bar. The bar can be dropped in case of laminar flow.

It is assumed that the Reynolds number and the Péclet number are very large, whereas the Prandtl number is of the order of 1, i.e.,

$$Re = u_{\infty}L/\nu \gg 1, \quad Pe = u_{\infty}L/\alpha \gg 1, \quad Pr = \nu/\alpha = O(1), \quad (1)$$

where L is the plate length, u_∞ is the constant free-stream velocity far upstream of the plate, and ν and α are the fluid's kinematic viscosity and thermal diffusivity, respectively, which are assumed to be constant. For justification of assuming constant fluid properties in contrast to accounting for variable fluid properties see [22], pp. 81-96, for a general discussion and [23,24] for applications.

A Cartesian coordinate system (x,y) is used, with the x -axis coinciding with the dividing streamline $\Psi = 0$, see Fig. 1. In general, the x -axis deviates from the plane of the plate, depending on the whole flow field, see, for instance, Fig. 10 of [13] or Fig. 3 of [4].

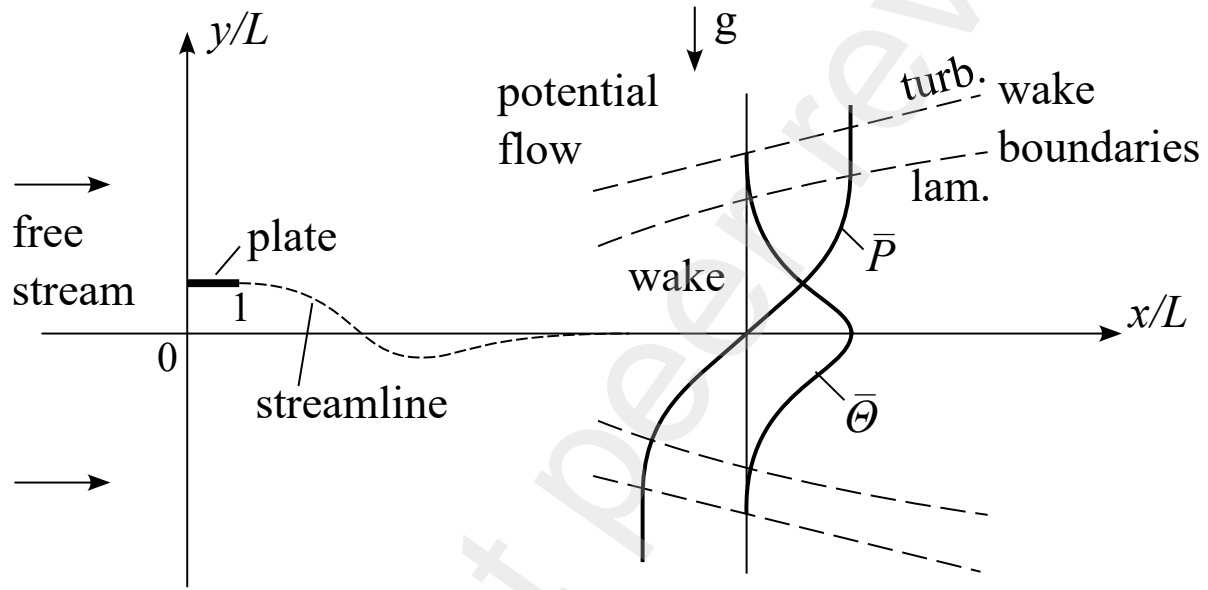


Fig. 1. The horizontal wake flow far downstream of a horizontal plate with profiles of temperature perturbation ($\bar{\theta}$) and pressure perturbation (\bar{P}) (schematic).

Dimensionless variables are then introduced as follows:

$$X = x/L, \quad Y = y/L, \quad (2)$$

$$\bar{U} = \bar{u}/u_\infty, \quad \bar{V} = \bar{v}/u_\infty, \quad (3)$$

$$\bar{\theta} = \rho_\infty c_p u_\infty L (\bar{T} - T_\infty) / \dot{Q}, \quad \bar{P} = (\bar{p} - p_\infty) / \rho_\infty u_\infty^2, \quad (4)$$

where u , v , T and p are, in this order, the velocity components in direction of x and y , respectively, the absolute temperature and the pressure. T_∞ and ρ_∞ are the constant values of temperature T and mass density ρ , respectively, in the free stream, c_p is the fluid's isobaric specific heat capacity, which is assumed to be constant, \dot{Q} is the total heat flow from the plate per units of time and depth of the plane flow, respectively, and p_∞ is the hydrostatic pressure in the undisturbed fluid. The total heat flow rate \dot{Q} may be positive or negative, depending on whether the plate is heated or cooled. The hydrostatic pressure varies in vertical direction due to the gravity force g per unit mass. There are, of course, other possibilities to define

dimensionless variables, in particular for the temperature, but the present choice leads to formally simple results.

3. Boundary-layer equations for the dimensionless variables

Considered is the far wake, which is characterized by very large distances from the plate, i.e. $X \rightarrow \infty$. Following the classical estimates for laminar flows at large Reynolds numbers it can be seen that the laminar horizontal far wake is slender and satisfies the conditions for applying the boundary-layer theory. Regarding the turbulent far wake, it is known from experiments that most turbulent free shear layers are sufficiently slender to allow the application of the boundary-layer theory, cf. [25] for a survey. Here we will follow that common practice, cf. [6], p. 655. A posteriori (Section 6.3) it will be seen that an effective buoyancy parameter must not be too large in order not to violate the assumption of slenderness. The width of the turbulent far wake even tends to zero in the limiting case of very weak buoyancy effects (Section 6.4).

For formulating the basic equations, further common assumptions are made. Dissipation and the work done by pressure are neglected in the thermal energy equation. Justification of that simplification is not as trivial as it might appear at the first glance, cf. Appendix A. Furthermore, the Boussinesq approximation is applied, cf. [6], pp. 88-89, and the discussion in [22], p. 60. Finally, in case of turbulent flow it is assumed that density fluctuations are negligible, cf. [6], p. 616. On the basis of those assumptions, we obtain the following boundary-layer equations in terms of the dimensionless variables introduced according to Eqs. (2) to (4):

$$\frac{\partial \bar{U}}{\partial X} + \frac{\partial \bar{V}}{\partial Y} = 0, \quad (5)$$

$$\bar{U} \frac{\partial \bar{U}}{\partial X} + \bar{V} \frac{\partial \bar{U}}{\partial Y} + \frac{\partial \bar{P}}{\partial X} = \frac{\partial}{\partial Y} \left[\left(\frac{1}{\text{Re}} + \frac{1}{\text{Re}_t} \right) \frac{\partial \bar{U}}{\partial Y} \right], \quad (6)$$

$$\frac{\partial \bar{P}}{\partial Y} = \text{Ri} \bar{\theta}, \quad (7)$$

$$\bar{U} \frac{\partial \bar{\theta}}{\partial X} + \bar{V} \frac{\partial \bar{\theta}}{\partial Y} = \frac{\partial}{\partial Y} \left[\left(\frac{1}{\text{Pe}} + \frac{1}{\text{Pe}_t} \right) \frac{\partial \bar{\theta}}{\partial Y} \right], \quad (8)$$

where

$$\text{Ri} = g\beta_p \dot{Q} / \rho_\infty c_p u_\infty^3 \quad (9)$$

is the Richardson number [12,13]. The Richardson number may be positive or negative, depending on whether the plate is heated or cooled. The isobaric thermal expansivity β_p of the fluid is assumed to be a positive constant, as usual with the Boussinesq approximation. The special case of vanishing β_p is excluded here; it would require a more complicated analysis [26]. The ‘‘turbulent’’ Reynolds number, the ‘‘turbulent’’ Péclet number and, for later use, the ‘‘turbulent’’ Prandtl number are defined in analogy to Eq. (1) as

$$\text{Re}_t = u_\infty L / \nu_t, \quad \text{Pe}_t = u_\infty L / \alpha_t, \quad \text{Pr}_t = \nu_t / \alpha_t, \quad (10)$$

with ν_t and α_t as turbulent kinematic viscosity and turbulent thermal diffusivity, respectively. Owing to the character of turbulent flow, Re_t , Pe_t and Pr_t are, unlike Re , Pe and Pr , not

constant parameters that govern the flow, but rather dimensionless representations of the flow variables v_t and α_t .

Y is to be taken as a boundary-layer coordinate. For laminar flow with large Reynolds numbers, Y is stretched with $\sqrt{\text{Re}}$, and matching with the outer, potential flow is accomplished with $\hat{Y} = \sqrt{\text{Re}} Y \rightarrow \pm \infty$. For turbulent flow, the edges of the wake are described by $y = b^\pm(x)$ or $Y = B^\pm(X)$, with $B^\pm(X) = L^{-1}b^\pm(x)$. The upper and lower signs refer to the upper and lower side, respectively, of the wake. The dimensionless width of the wake is then $B(X) = B^+(X) - B^-(X)$, and the slenderness of the wake is expressed by $B(X) \ll X$.

Apart from the common terms due to convection and shear stresses, respectively, Eq. (6) contains a pressure term that represents the indirect effect of buoyancy in horizontal flows. As Eq. (7) shows, the pressure term stems from the hydrostatic pressure perturbation that is caused by the temperature perturbation. The hydrostatic pressure perturbation is seen to be proportional to the Richardson number, Ri . Since the present investigation aims at describing wake flows with substantial buoyancy effects, it is assumed that $\text{Ri} = O(1)$, with the limiting case $\text{Ri} \rightarrow 0$ to be considered separately in Section 6.4 of the paper.

It might be of interest to note that the Richardson number is related to the Archimedes number Ar , which is sometimes used in other investigations, e.g. [11], as follows:

$$\text{Ar} = gL\beta_p\dot{Q}/ku_\infty^2 = \text{Ri Pe} . \quad (11)$$

To ensure that the wake is horizontal, we require that the dividing streamline, which separates the upper part of the wake from the lower one and coincides with the x -axis, is horizontal. This gives the boundary condition

$$\bar{V} = 0 \text{ at } Y = 0 . \quad (12)$$

Since there is no temperature disturbance in the outer, potential flow, the temperature disturbance in the wake has to decay according to the boundary condition

$$\bar{\theta} = 0 \begin{cases} \text{as } \hat{Y} \rightarrow \pm \infty \text{ for laminar flow,} \\ \text{at } Y = B^\pm(X) \text{ for turbulent flow.} \end{cases} \quad (13)$$

Finally we have to consider the condition for matching the wake flow with the potential flow, in which Bernoulli's equation is valid. According to Eq. (4), the pressure disturbance \bar{P} is defined, in terms of dimensionless variables, as the deviation from the hydrostatic pressure in the undisturbed fluid outside the wake. Thus, Bernoulli's equation without a gravity term is applied to obtain the matching condition for the wake as follows:

$$\bar{P} = (1/2)(1 - \bar{U}^2) \begin{cases} \text{as } \hat{Y} \rightarrow \pm \infty \text{ for laminar flow,} \\ \text{at } Y = B^\pm(X) \text{ for turbulent flow.} \end{cases} \quad (14)$$

Eq. (14) permits positive as well as negative values of \bar{P} on either side of the wake. However, integrating Eq. (7) over the wake cross section gives

$$\begin{cases} \bar{P}(X, +\infty) - \bar{P}(X, -\infty) = (\text{Ri}/\sqrt{\text{Re}}) \int_{-\infty}^{+\infty} \bar{\theta} d\hat{Y} \text{ for laminar flow,} \\ \bar{P}(X, B^+) - \bar{P}(X, B^-) = \text{Ri} \int_{B^-}^{B^+} \bar{\theta} dY \text{ for turbulent flow,} \end{cases} \quad (15)$$

indicating that there is a hydrostatic pressure jump across the wake. This pressure jump has to be compensated by the potential flow. In outer variables, i.e. from the point of view of the

potential flow, the wake appears infinitesimally thin, and the pressure jump has to be compensated by a vortex sheet. This has already been elaborated in previous work [11–13] for weak buoyancy effects, i.e. small values of Ri , and it is equally valid in the present case. Thus, the deviation of the longitudinal velocity component from the free-stream value has to be antisymmetric as the boundaries of the wake are approached, leading to the following additional matching conditions for the wake:

$$\begin{cases} \bar{U}(X, +\infty) - 1 = -[\bar{U}(X, -\infty) - 1] & \text{for laminar flow,} \\ \bar{U}(X, B^+) - 1 = -[\bar{U}(X, B^-) - 1] & \text{for turbulent flow.} \end{cases} \quad (16)$$

Note that applying Bernoulli's equation implies a coupling (interaction) between the wake flow and the potential flow; cf. also the interaction problem investigated in [19].

The set of equations now consists of the 6th order parabolic system of differential equations (5) to (8) and the boundary conditions Eqs. (12) to (14) and (16), where Eqs. (13) and (14) count for two boundary conditions each. Summing up, the appropriate number of 6 boundary conditions is obtained. However, as the thermal energy equation, Eq. (8), is homogenous and, furthermore, the associated boundary condition Eq. (13) is also homogeneous, the over-all thermal energy balance will have to be considered to fix the maximum value of the temperature perturbation.

4. Over-all thermal energy balance

As the Péclet number is assumed to be very large according to Eq. (1), the heat flow due to conduction in main flow direction is negligible in comparison to the enthalpy flow. The over-all thermal energy balance then reduces to

$$\dot{Q} = \rho_{\infty} c_p \int_{\text{wake}} (\bar{T} - T_{\infty}) \bar{u} dy = \text{const} , \quad (17)$$

where the integral is to be taken over any cross section of the wake. Introducing the dimensionless variables according to Eqs. (2) to (4), one obtains

$$\begin{cases} (1/\sqrt{\text{Re}}) \int_{-\infty}^{+\infty} \bar{\theta} \bar{U} d\hat{Y} = 1 & \text{for laminar flow,} \\ \int_{B^-}^{B^+} \bar{\theta} \bar{U} dY = 1 & \text{for turbulent flow.} \end{cases} \quad (18)$$

The formal simplicity of Eqs. (18) indicates that the choice of $\dot{Q}/\rho_{\infty} c_p u_{\infty} L$ as a reference temperature in Eq. (4) is a convenient one.

5. The laminar horizontal wake

5.1 Boundary-layer equations for stretched variables

For laminar flow, averaging is not required, i.e. the bars over all variables are to be dropped. Furthermore, the terms containing Re_t and Pe_t vanish in Eqs. (6) and (8), respectively. In accordance with boundary-layer theory, the lateral coordinate Y and the lateral velocity component V are stretched as follows:

$$\hat{Y} = \sqrt{\text{Re}} Y , \quad \hat{V} = \sqrt{\text{Re}} V . \quad (19)$$

The stretched coordinate \hat{Y} was already used in sections 3 and 4. To satisfy the continuity equation, Eq. (5), a stream function Ψ is introduced with the relations

$$U = \Psi_{\hat{Y}}, \quad \hat{V} = -\Psi_X. \quad (20)$$

Here, and in what follows, partial derivatives with respect to X and \hat{Y} are indicated by the respective subscripts. The momentum equations, Eqs. (6) and (7), and the thermal energy equation, Eq. (8), then become:

$$\Psi_{\hat{Y}}\Psi_{X\hat{Y}} - \Psi_X\Psi_{\hat{Y}\hat{Y}} + P_X = \Psi_{\hat{Y}\hat{Y}\hat{Y}}, \quad (21)$$

$$P_{\hat{Y}} = (\text{Ri}/\sqrt{\text{Re}})\theta, \quad (22)$$

$$\Psi_{\hat{Y}}\theta_X - \Psi_X\theta_{\hat{Y}} = \text{Pr}^{-1}\theta_{\hat{Y}\hat{Y}}. \quad (23)$$

5.2 Similarity transformation

Very far downstream of the plate the details of the flow at the plate are not of importance, and the flow can be expected to exhibit spatial self-similarity. It might then be tempting to apply the similarity transformation known from classical wake solutions, cf. [6], pp. 187-190, 218-222. This, however, would be misleading in case of substantial buoyancy effects, i.e. if $P_{\hat{Y}} = O(1)$. As a consequence of the pressure term P_X , which is due to buoyancy according to Eq. (7), the momentum equation (6) cannot be satisfied with the similarity transformation applicable to the non-buoyant wake. However, the present problem is related to the problem of a semi-infinite horizontal plate that is thermally isolated with the exception of the leading edge, where there is a heat source or a heat sink. This problem was investigated in [27]. Guided by [27], the similarity transformation that will turn out to be suitable for the present problem is written as follows:

$$\xi = X; \quad \eta = \hat{Y}/\sqrt{X}, \quad (24)$$

$$\Psi = \xi^{1/2}f(\eta), \quad (25)$$

$$\theta = \xi^{-1/2}g(\eta), \quad (26)$$

$$P = g(\eta). \quad (27)$$

For later use, the velocity components are of interest. Eq. (25) gives

$$U = \Psi_{\hat{Y}} = f'(\eta), \quad (28)$$

$$\hat{V} = -\Psi_X = (1/2)\xi^{-1/2}[\eta f'(\eta) - f(\eta)]. \quad (29)$$

Here, and in what follows, primes indicate derivatives.

With Eq. (27) for P , the pressure jump across the wake according to Eq. (15) becomes independent of X , leading to a constant vorticity distribution in the vortex sheet of the potential flow. This requires care with formulating proper boundary conditions for the potential-flow equations, as discussed in previous work [11–13,16–18].

5.3 Ordinary differential equations and boundary conditions

Transforming Eqs. (21) to (23) according to Eqs. (24) to (27) gives a set of ordinary differential equations for f , g and ϑ . Eq. (23) is homogeneous and linear with respect to ϑ . Furthermore, the boundary conditions (13) are also homogeneous. Thus, one can introduce a normalized temperature disturbance $\tilde{\vartheta}$ by the relation

$$\vartheta = C_{\theta} \tilde{\vartheta}, \quad (30)$$

together with the boundary condition

$$\tilde{\vartheta}(0) = 1. \quad (31)$$

C_{θ} is a free constant that will be determined from the over-all thermal energy balance considered below. The following set of ordinary differential equations is then obtained:

$$2f''' + ff'' + \tilde{K}\eta\tilde{\vartheta} = 0, \quad (32)$$

$$g' = \tilde{K}\tilde{\vartheta}, \quad (33)$$

$$(2/\text{Pr})\tilde{\vartheta}'' + f\tilde{\vartheta}' + f'\tilde{\vartheta} = 0, \quad (34)$$

with the “effective buoyancy parameter”

$$\tilde{K} = C_{\theta}\text{Ri}/\sqrt{\text{Re}}. \quad (35)$$

According to Eq. (33), buoyancy is a first-order effect if $\tilde{K} = O(1)$. Not surprisingly, Eqs. (32) and (34) are formally identical with the equations (11a) and (11b), respectively, of [27].

The boundary conditions and the matching conditions, Eqs. (12) to (16) transform into the following set of equations:

$$f(0) = 0, \quad (36)$$

$$\tilde{\vartheta} = 0 \text{ as } \eta \rightarrow \pm \infty, \quad (37)$$

$$g = (1/2)[1 - (f')^2] \text{ as } \eta \rightarrow \pm \infty, \quad (38)$$

$$[f'(+\infty) - 1] = -[f'(-\infty) - 1]. \quad (39)$$

Eqs. (36) to (39) are 6 boundary conditions for the 6th-order system of differential equations, Eqs. (32) to (34). Since the differential equation (34) as well as the boundary conditions according to Eq. (37) are homogeneous, the normalizing condition Eq. (31) has to be obeyed in order to fix the maximum value of the temperature perturbation.

Eq. (34) can be integrated once. Making use of the boundary condition (37), and anticipating exponential decay of the temperature perturbation with $\eta \rightarrow \pm \infty$, cf. Appendix B, the result becomes

$$(2/\text{Pr})\tilde{\vartheta}' + f\tilde{\vartheta} = 0. \quad (40)$$

A formal solution of this first-order differential equation subject to the normalizing boundary condition (31) can be given as follows:

$$\tilde{\vartheta} = \exp\left(-\frac{\text{Pr}}{2} \int_0^{\eta} f d\eta\right). \quad (41)$$

Whether applying Eq. (41) is preferable to using the differential equation (40) with the normalizing boundary condition (31) is a matter of taste. In case of using Eq. (40) for a numerical solution it is of interest that the boundary conditions according to Eq. (37) will be automatically satisfied, as the formal analytical solution (41) shows.

Finally, Eq. (33) can also be formally integrated, with the result

$$g = \tilde{K} \int_{\eta^*}^{\eta} \tilde{\vartheta} d\eta, \quad (42)$$

where η^* is a constant that is to be determined as part of the solution. Note that $\eta = \eta^*$ gives the position of vanishing pressure perturbation.

The buoyancy parameter \tilde{K} , as well as the Richardson number Ri , can be positive or negative for a heated or cooled body, respectively. The system of differential equations (32) to (34) is, however, symmetric with respect to the change of signs of \tilde{K} and η . Therefore, only positive values of \tilde{K} , corresponding to a heated body, will be considered. Results for a cooled body can be obtained by simply reverting the direction of the η -axis.

It remains to determine the constant C_{θ} , which is required to obtain the temperature disturbance associated with a certain over-all heat flow by applying Eq. (30). Inserting the transformed variables into the upper equation of Eqs. (18) gives

$$C_{\theta}^{-1} = (1/\sqrt{Re}) \int_{-\infty}^{+\infty} \tilde{\vartheta} f' d\eta. \quad (43)$$

A further equation for C_{θ} can be obtained from Eq. (43) with an integration by parts, substituting for $\tilde{\vartheta}'$ in the integral according to Eq. (40), and observing the boundary condition Eq. (37), thereby anticipating that the temperature perturbation decays exponentially; see Appendix B for verification. The result is the following:

$$C_{\theta}^{-1} = (Pr/2\sqrt{Re}) \int_{-\infty}^{+\infty} \tilde{\vartheta} f^2 d\eta. \quad (44)$$

As $\tilde{\vartheta} > 0$ according to Eq. (41), the integral in Eq. (44) is also positive. Thus C_{θ} is positive, as required.

The analysis of the asymptotic behavior of the solutions as $\eta \rightarrow \pm \infty$, which is given in Appendix B, is not only useful for deriving Eq. (44), it also shows that there is no reversed flow at the wake boundaries.

5.4 Numerical solutions for the laminar wake

5.4.1 Method of solution

The system of differential equations (32), (33) and (40) with the boundary conditions (31) and (36) to (39) is solved with the shooting method, implemented in the numerical differential-equation solver “NDSolve” of Wolfram Mathematica, version 13.3. For that purpose Eq. (32) is transformed into an equivalent system of three first-order differential equations which are numerically integrated together with Eqs. (33) and (40) from the initial point $\eta = 0$ in both directions, using Eqs. (31) and (36) as initial conditions. The three remaining unknown initial values $f'(0)$, $f''(0)$ and $g(0)$ are computed iteratively to satisfy the three asymptotic matching conditions of Eqs. (38) and (39) at large, but finite, distances from the axis, i.e. at

$\eta = \eta_b^- < 0$ and $\eta = \eta_b^+ > 0$. To ensure that the boundary conditions at finite distances are indeed approximating the asymptotic matching conditions, it is advisable to prescribe the following additional boundary conditions:

$$f''(\eta_b^\pm) = 0, \quad (45)$$

where η_b^\pm stands for η_b^+ and η_b^- , respectively. We found the values $\eta_b^- = -15$ and $\eta_b^+ = 15$ to be sufficient. In order to enforce the artificial boundary condition (45), the numerical solution is sought in the least-norm sense. The L_1 norm of the residuals of all boundary conditions is required to be smaller than a prescribed numerical tolerance of 10^{-5} .

5.4.2 Non-uniqueness of the solution

Depending on the initial guess for the shooting method, we find two different kinds of the solution which co-exist within a certain parameter range. The solutions of the first kind, considered in section 5.4.3, are characterized by a monotonous variation of the horizontal velocity component f' . In contrast, the solutions of the second kind, which will be discussed in section 5.4.4, are characterized by non-monotonous f' . The solutions of the second kind exhibit flow reversal within part of the wake's cross-section, even though the horizontal velocity component in the outer flow remains non-negative (see Appendix B).

5.4.3 Solutions of the first kind

The solution of the first kind is obtained when the initial conditions corresponding to the non-buoyant solution, $f'(0) = 1$, $f''(0) = 0$ and $g(0) = 0$, are employed as an initial guess for the shooting method. For $\tilde{K} = 1/4$ and $\text{Pr} = 1$, the solution converges to the initial conditions $f'(0) = 1.05$, $f''(0) = -0.126$ and $g(0) = -0.115$. The resulting profiles are shown in Fig. 2. The value of the temperature normalization constant is $C_\theta = 0.278\sqrt{\text{Re}}$, leading to the value $\text{Ri} = 0.899$ for the Richardson number. For these parameters, the horizontal velocity component at the boundaries of the wake is $f'(\pm\infty) = 1 \mp 0.435$.

In the wake the horizontal velocity component varies monotonously between the boundary values. Although the perturbation $f' - 1$ of the outer horizontal velocity component is antisymmetric about $\eta = 0$, the antisymmetry is broken inside the wake, which is evident from the observation that $f'(0) \neq 1$. For the solution of the first kind, the horizontal velocity component at the zero streamline $\eta = 0$ is always larger than one. The vertical velocity component, $\eta f' - f$, is negative at both sides of the wake. It vanishes at $\eta = 0$, such that the zero streamline remains horizontal, cf. Eq. (12).

The profile of the temperature perturbation $\tilde{\vartheta}$ resembles, at the first sight, the classical non-buoyant solution, cf. [6], pp. 187-190 and 218-219. Its symmetry about $\eta = 0$ is, however, broken due to the asymmetric horizontal velocity component. The temperature profile is wider in the upper part of the wake, where the horizontal velocity component is reduced, and narrower in the lower part, where the horizontal velocity component is larger. The broken symmetry of the temperature profile causes the broken antisymmetry of the profile of the horizontal velocity component.

Due to the nonlinearity of the Bernoulli equation, cf. Eq. (38), the pressure perturbation g is not even antisymmetric at the boundaries. The boundary values are $g(\infty) = 0.341$ and $g(-\infty) = -0.530$. The profile of g crosses zero at $\eta = \eta^* = 0.471$.

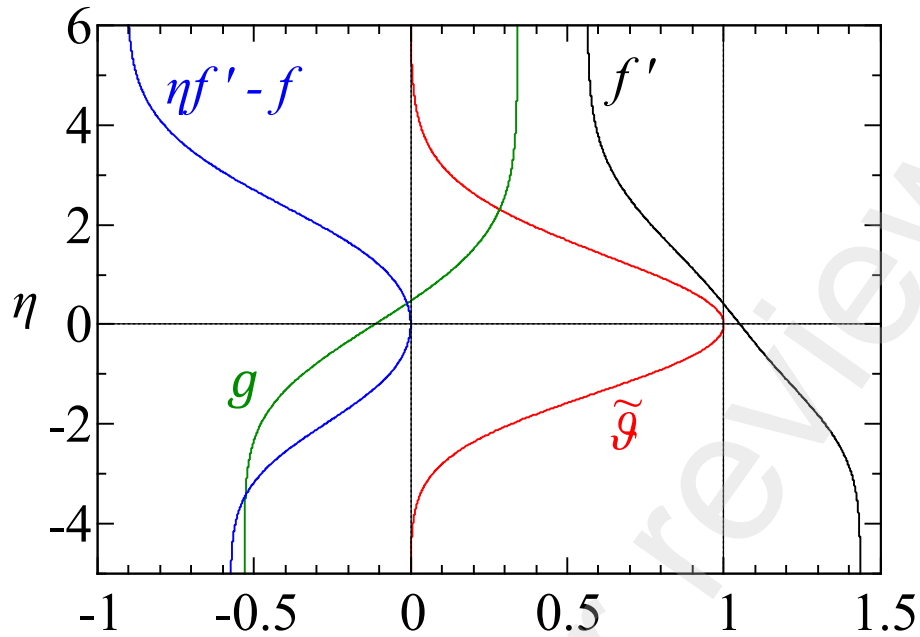


Fig. 2. A solution of the first kind: Profiles of horizontal velocity component f' (black), normalized temperature perturbation $\tilde{\vartheta}$ (red), pressure perturbation g (green) and vertical velocity component $\eta f' - f$ (blue). $\tilde{K} = 1/4$, $\text{Pr} = 1$.

The solution of the first kind exists up to a critical value of \tilde{K} , depending on Pr . For $\text{Pr} = 1$, the critical value is $\tilde{K}_c = 0.61$. The corresponding critical Richardson number is 2.31. At the critical value, the horizontal velocity component vanishes at the upper boundary. According to Eq. (39) the horizontal velocity component at the lower boundary is $f'(-\infty) = 2$. The boundary values of the pressure perturbation then follow from Eq. (38) as $g(-\infty) = -3/2$ and $g(\infty) = 1/2$. A further increase of \tilde{K} beyond the critical value would require the horizontal velocity component to become negative at the upper boundary, which is forbidden as it would lead to an exponential growth of temperature, cf. Eq. (B.4).

5.4.4 Solutions of the second kind, reversed flow regimes

The solution of the second kind is obtained when the initial guess for $f'(0)$ is below a certain threshold, depending on the parameters \tilde{K} and Pr . For example, the default initial guess $f'(0) = 0$ of the solver typically lies inside the basin of attraction of the solution of the second kind. For $\text{Pr} = 1$ and $\tilde{K} = 0.04$, the solution of the second kind is shown in Fig. 3. The main difference compared to the solution of the first kind is a reversed flow region in the wake. Note that the perturbation of the horizontal velocity component in the reversed-flow region remains of the order of 1 even for such small values of \tilde{K} as in Fig. 3.

Since, according to Eq. (4), the same reference quantities are used, and, furthermore, the same boundary conditions are applied irrespective of whether the flow is in forward direction or reversed, it is tacitly assumed that the stagnation pressure far downstream is the same as far upstream.

Due to the reduced horizontal velocity component in the lower part of the wake, the temperature perturbation profile is wider in the lower part than in case of the solution of the first kind. For $\tilde{K} < 0.06$, the temperature profile contains a second local maximum below the dividing streamline. When \tilde{K} decreases, the region of the reversed flow grows, as well as the distance between the temperature maxima.

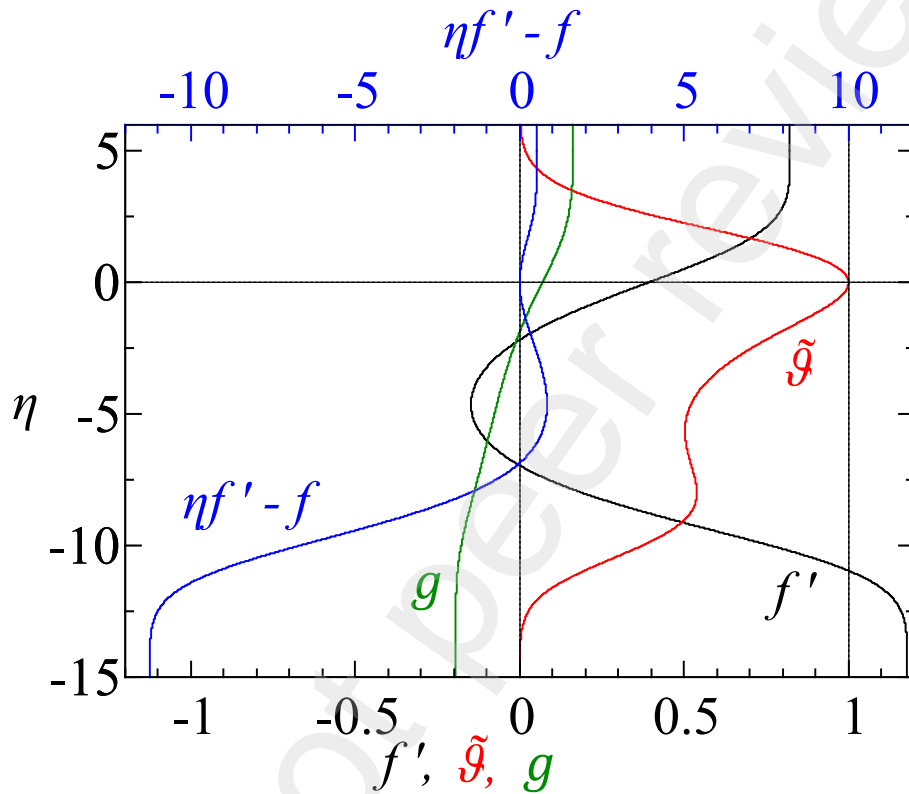


Fig. 3. A solution of the second kind: Profiles of flow quantities, distinguished by color. $\tilde{K} = 0.04$, $Pr = 1$.

The vertical velocity component is positive at the upper boundary and negative at the lower boundary. Note that in the lower part of the wake, the vertical velocity component changes sign at the same point as the horizontal velocity component. Therefore, on the lower side, fluid is released into the outer flow only from the lower layer of the wake with a positive horizontal velocity component. From the reversed-flow region, on the other hand, fluid is transported towards the dividing streamline at $\eta = 0$.

For $Pr = 1$, the solution of the second kind is found for $\tilde{K} \leq 0.27$, corresponding to $Ri \leq 0.734$. Again, the upper bound for \tilde{K} corresponds to vanishing horizontal velocity component at the upper boundary of the wake. The critical value of \tilde{K} is lower as compared to the solution of the first kind, because the wider temperature profile leads to a larger pressure jump across the wake for the same value of \tilde{K} , cf. Eq. (42).

5.4.5 Entrainment

The entrainment of mass into the wake is described by the lateral (i.e. vertical) velocity component, cf. Appendix B, Eq. (B.13). Numerical results for solutions of the first kind show that entrainment of mass is positive on the upper side and negative on the lower side. For the solution of the first kind, the net entrainment is positive, i.e., the mass flow in the wake increases with increasing distance from the origin. However, for the solution of the second kind, the entrainment is negative on both sides. Those first-order results would have to be taken into account in a second-order solution for the potential flow and the wake, which is beyond the scope of the present work.

5.4.6 Limitations to the parameter regime

As indicated above for the solutions of both the first and the second kind, no numerical solution could be found for values of the buoyancy parameter above an upper bound, depending on the Prandtl number. This resembles the critical value found in [16] for the interaction between the vortex line that represents the wake and the induced potential flow. In our case, the upper bound corresponds to vanishing horizontal velocity component at the upper boundary, since the solution exists only for non-negative velocity in the outer flow. We expect that for supercritical values of \tilde{K} the self-similar structure of the wake, described by Eqs. (24) to (27), is broken. This hypothesis is subject to being confirmed by solutions of the full Navier-Stokes equations.

6. The turbulent horizontal wake

6.1 Similarity transformation of the equations of motion

The set of basic equations now consists of the continuity equation (5), the momentum equations (6), (7) and the thermal energy equation (8). To satisfy the continuity equation (5), a stream function $\bar{\Psi}$ is introduced with the relations

$$\bar{U} = \bar{\Psi}_Y, \quad \bar{V} = -\bar{\Psi}_X. \quad (46)$$

For sufficiently large Reynolds and Péclet numbers the molecular viscosity, ν , and the molecular thermal diffusivity, α , can be neglected in comparison to the turbulent viscosity, ν_t , and the turbulent thermal diffusivity, α_t , respectively. Thus, the terms $1/\text{Re}$ and $1/\text{Pe}$ are dropped in Eqs. (6) and (8), respectively.

With those simplifications, the equations governing the turbulent horizontal far wake do not contain a characteristic length as a parameter. It follows from dimensional analysis that the width of the far wake has to be proportional to the distance from the plate. Thus, the dimensionless width of the wake is written as $B = C_B X$ in terms of the dimensionless coordinate system (X, Y) , with $C_B = \text{const}$. This is in contrast to the classical, non-buoyant wake [6], pp. 669-671.⁵ For the turbulent shear layer to be slender, it is required that $C_B \ll 1$. But in view of the terms that are neglected in the boundary-layer equations, a more appropriate criterion for the applicability of the boundary-layer equations stems from the

⁵ The non-buoyant turbulent wake contains the length of the plate as a parameter, which enters the basic equations via the drag force per unit depth, i.e. $c_D L \rho_\infty u_\infty^2 / 2$, with c_D as the drag coefficient.

magnitude of the lateral velocity component, i.e. $\bar{V} \ll 1$ may serve as a sufficient and necessary condition.

In accord with the linear growth rate of the wake, the following similarity transformation is applied:

$$\xi = X ; \zeta = Y/X , \quad (47)$$

$$\bar{\Psi} = \xi \bar{f}(\zeta) , \quad (48)$$

$$\bar{\theta} = \xi^{-1} \bar{\vartheta}(\zeta) , \quad (49)$$

$$\bar{P} = \bar{g}(\zeta) , \quad (50)$$

$$1/\text{Re}_t = \nu_t/u_\infty L = \xi \bar{n}(\zeta) , \quad (51)$$

$$1/\text{Pe}_t = \alpha_t/u_\infty L = \xi \bar{a}(\zeta) . \quad (52)$$

Representing the dimensionless width of the wake as $B = C_B X$ is achieved by writing $\zeta = \zeta_B^+$ and $\zeta = \zeta_B^-$ for the upper and lower wake edges, respectively, and imposing the condition

$$\zeta_B^+ - \zeta_B^- = C_B \quad (53)$$

on the constants ζ_B^+ , ζ_B^- and C_B . Thus, the equations for the upper and lower edges of the wake, i.e. $Y = B^\pm(X)$, can be written as $Y = \zeta_B^+ X$ and $Y = \zeta_B^- X$, respectively. The constants ζ_B^+ , ζ_B^- and C_B have to be found in course of the numerical solutions, cf. below.

According to the definitions of Re_t , Pe_t and Pr_t in Eq. (10), the dimensionless turbulent kinematic viscosity, \bar{n} , and the dimensionless turbulent thermal diffusivity, \bar{a} , are related to each other as

$$\bar{a} = \bar{n}/\text{Pr}_t . \quad (54)$$

For non-buoyant mixing layers and non-buoyant wakes, see [6], pp. 668 and 670, respectively, the value $\text{Pr}_t = 0.5$ is recommended for the turbulent Prandtl number. However, buoyancy in horizontal, or nearly horizontal, turbulent shear layers may affect the turbulent Prandtl number, as discussed in [28], p. 378. According to an empirical relationship given in [29], p. 19, the effect is small for sufficiently small Richardson numbers. It will turn out that the magnitude of the Richardson number is rather limited if the solutions are required to satisfy the condition of slenderness of the wake. Thus, the effect of buoyancy on the turbulent Prandtl number is neglected and the constant value $\text{Pr}_t = 0.5$ will be taken for the numerical solutions.

Of particular interest are the velocity components in the self-similar flow field, which become:

$$\bar{U} = \bar{\Psi}_Y = \bar{f}'(\zeta) , \quad (55)$$

$$\bar{V} = -\bar{\Psi}_X = \zeta \bar{f}'(\zeta) - \bar{f}(\zeta) . \quad (56)$$

According to Eq. (49) the temperature perturbation decays more rapidly with increasing distance from the plate as compared to the classical solution for the wake without buoyancy. The opposite is true for the perturbation of the longitudinal velocity component, which is

constant in the present case, whereas it decays in the buoyancy-free wake; cf. [6], pp. 669-671.

Applying the similarity transformation, Eqs. (47) to (52), (55) and (56), to the momentum equations (6) and (7) and the thermal energy equation (8) gives a set of ordinary differential equations. As in the case of laminar flow, cf. Eqs. (30) and (31), a normalized temperature disturbance $\tilde{\vartheta}$ is introduced by the relation

$$\bar{\vartheta} = C_{\theta} \tilde{\vartheta}, \quad (57)$$

together with the boundary condition

$$\tilde{\vartheta}(0) = 1. \quad (58)$$

C_{θ} is again a free constant that will be determined from the over-all thermal energy balance considered below. The following set of ordinary differential equations is then obtained:

$$\bar{f}\bar{f}'' + \zeta\bar{g}' = -(\bar{n}\bar{f}'')', \quad (59)$$

$$\bar{g}' = \tilde{Ri}\tilde{\vartheta}, \quad (60)$$

$$\bar{f}\tilde{\vartheta}' + \bar{f}'\tilde{\vartheta} = -(\bar{a}\tilde{\vartheta}')'. \quad (61)$$

The parameter \tilde{Ri} is an effective Richardson number defined as $\tilde{Ri} = C_{\theta} Ri$.

Of course, \bar{g} can be eliminated from the set of differential equations by inserting Eq. (60) into Eq. (59). To eliminate \bar{g} also from the boundary conditions, Eq. (60) is formally integrated with the result

$$\bar{g}(\zeta) = \bar{g}(\zeta_B^-) + \tilde{Ri} \int_{\zeta_B^-}^{\zeta} \tilde{\vartheta} d\zeta. \quad (62)$$

The boundary conditions have been formulated in Section 3. They have to be expressed in terms of the variables of the self-similar flow as defined in Eqs. (47) to (50), (55) and (56). In addition to Eq. (58), one obtains

$$\bar{f}(0) = 0 \quad (63)$$

from Eq. (12) as a further boundary condition at the x -axis. At the edges of the wake the following boundary conditions are obtained from Eqs. (13), (14) and (16), with ζ_B^{\pm} standing for ζ_B^+ or ζ_B^- :

$$\tilde{\vartheta}(\zeta_B^{\pm}) = 0, \quad (64)$$

$$2\bar{g}(\zeta_B^{\pm}) = 1 - [\bar{f}'(\zeta_B^{\pm})]^2, \quad (65)$$

$$[\bar{f}'(\zeta_B^+) - 1] = -[\bar{f}'(\zeta_B^-) - 1]. \quad (66)$$

Owing to the non-linearity of the Bernoulli equation, Eq. (65) is non-linear. This would be a disadvantage for the numerical solutions. However, by some algebraic manipulations of Eqs. (65) and (66), and with the help of Eq. (62), the following linear boundary conditions can be obtained:

$$\bar{f}'(\zeta_B^{\pm}) = 1 \mp (1/2)\tilde{Ri} \int_{\zeta_B^-}^{\zeta_B^{\pm}} \tilde{\vartheta} d\zeta, \quad (67)$$

where the upper and lower signs, respectively, on the right-hand side correspond to those on the left-hand side. How the integral relationships Eqs. (62) and (67) can be of advantage for the numerical solutions will be described in Section 6.3.

A smooth transition from the turbulent wake to the potential flow, as required by matching, is obtained if the gradients of the turbulent mean values vanish at the wake edges, i.e.

$$\bar{f}''(\zeta_B^\pm) = 0 \quad (68)$$

and

$$\tilde{\vartheta}'(\zeta_B^\pm) = 0. \quad (69)$$

It is now convenient to integrate Eq. (61) once and eliminate the constant of integration by applying the boundary conditions (64) and (69) to obtain:

$$\bar{a}\tilde{\vartheta}' + \bar{f}\tilde{\vartheta} = 0. \quad (70)$$

Eq. (70) replaces Eq. (61) in the set of differential equations. Besides, it follows from Eq. (70) that a solution that satisfies the boundary condition Eq. (64) also satisfies the smoothness condition Eq. (69).

Finally, the lower Eq. (18), which expresses the over-all thermal energy balance, is written in terms of the similarity variables to obtain the following relation for the constant C_θ :

$$C_\theta^{-1} = \int_{\zeta_B^-}^{\zeta_B^+} \tilde{\vartheta}\bar{f}' d\zeta. \quad (71)$$

The value of C_θ is required to determine the real temperature disturbance from the normalized one with Eq. (57).

As in case of laminar flow, further insight into the qualitative properties of the solution can be gained by formally integrating the differential equation (70). Observing the normalizing condition, Eq. (58), one obtains:

$$\tilde{\vartheta} = \exp\left(-\int_0^\zeta (\bar{f}/\bar{a})d\zeta\right). \quad (72)$$

Furthermore, the integral in Eq. (71) is integrated by parts, $\tilde{\vartheta}'$ is replaced by $\tilde{\vartheta}$ according to Eq. (70), and the boundary conditions for $\tilde{\vartheta}$, i.e. Eq. (64), are used. The result is the following:

$$C_\theta^{-1} = \int_{\zeta_B^-}^{\zeta_B^+} (\tilde{\vartheta}/\bar{a})\bar{f}'^2 d\zeta. \quad (73)$$

According to Eq. (72) the temperature perturbation $\tilde{\vartheta}$ is positive in the whole cross section of the wake. Thus the integral in Eq. (73) is always positive. A further consequence of Eq. (72) will be discussed in the following section.

6.2 Equation for the turbulent kinetic energy and turbulence model equations

Closure of the system of equations requires turbulence modelling. Guided by previous experience [25,30], it appears promising to investigate the balance for the turbulent kinetic energy, k . For slender shear layers, the modelled balance equation for the turbulent kinetic energy can be written as follows, cf. [29], p. 22:

$$\bar{u} \frac{\partial k}{\partial x} + \bar{v} \frac{\partial k}{\partial y} = \nu_t \left(\frac{\partial \bar{u}}{\partial y} \right)^2 - \varepsilon + \frac{\partial}{\partial y} \left(\frac{\nu_t}{\sigma_k} \frac{\partial k}{\partial y} \right) - g \beta_p \alpha_t \frac{\partial \bar{T}}{\partial y}, \quad (74)$$

with

$$\nu_t = c_\mu l k^{1/2} \quad (75)$$

as the apparent turbulent viscosity,

$$\varepsilon = c_D l^{-1} k^{3/2} \quad (76)$$

as the turbulent dissipation rate⁶, and

$$l = c_l b \quad (77)$$

as a turbulence length, which may be interpreted as an integral length scale. The last term on the right-hand side of Eq. (74) is a modelled version of the buoyancy term in the k -equation, see [29], p. 22, with $-\alpha_t \partial \bar{T} / \partial y$ representing the lateral heat flux. Note that this term may be positive or negative, depending on the sign of $\partial \bar{T} / \partial y$. According to Eq. (77) the turbulence length is a fraction of the total width $b = b(x)$ of the free shear layer, with the edges of the free shear layer described by $y = b^\pm(x)$, i.e. $b = b^+(x) - b^-(x)$. This implies the common assumption that the turbulence length is constant in a cross section of the slender free shear layer. Various sets of the empirical parameters σ_k , c_μ , c_D and c_l can be found in the literature, cf. [6], pp. 560-561. In the present notation the empirical constant c_l combines two of the empirical parameters that are commonly used in the one-equation model. The following set, which is in accord with the conditions imposed by the asymptotic theory of slender free shear layers [25,31,32], has been chosen for the present work:

$$\sigma_k = 0.7, \quad c_\mu = 0.55, \quad c_D = 1, \quad c_l = 0.3. \quad (78)$$

For future comparisons with experiments it may be of interest to note that the modelling of the diffusion term, i.e. the third term on the right-hand side of Eq. (74), has been subject to criticism. Improvements have been proposed, see [6], p. 561, and the references given there.

In accord with the definitions of the dimensionless variables given in Eq. (3), the dimensionless turbulent kinetic energy, \bar{h} , is defined as

$$\bar{h}(\zeta) = k / u_\infty^2. \quad (79)$$

This relation, together with the similarity transformation according to Eqs. (47) to (52), (55) and (56) is introduced into Eq. (74), and the derivative $\tilde{\vartheta}'$ appearing in the buoyancy term is eliminated with the help of Eq. (70). This gives the following balance equation for the turbulent kinetic energy:

$$\bar{f} \bar{h}' + \bar{n} (\bar{f}'')^2 + \tilde{Ri} \bar{f} \tilde{\vartheta} - c_D c_l^{-1} \bar{h}^{3/2} + \sigma_k^{-1} (\bar{n} \bar{h}')' = 0, \quad (80)$$

with

$$\bar{n} = c_\mu c_l \bar{h}^{1/2}. \quad (81)$$

⁶ According to [6], p. 509, it would be appropriate, in contrast to common practice, to address ε as a ‘‘pseudo-dissipation’’ rate.

In the order of appearance, the physical meaning of the terms in Eq. (80) is the following: convection, production by turbulent shear stresses, production (positive or negative) by buoyancy forces, dissipation and diffusion. Eqs. (59) with (60) and Eq. (80) show that the buoyancy effects are of the order of 1 both in the momentum equations and in the turbulent kinetic energy balance if the effective Richardson number is of the order of 1.

The various terms in Eq. (80) may not always be of equal importance. A balance equation reduced to the second, the third and the fourth terms in Eq. (80) was already discussed in [28], p. 372. It is remarkable that a similar problem arises also in the absence of buoyancy, i.e. for $\bar{Ri} = 0$. It was already discussed in [33], pp. 215-217, and [34], pp. 104-145, that, under certain conditions, diffusion and convection of turbulent kinetic energy can be neglected, and the k-equation reduces to a balance of dissipation and production by turbulent shear stresses. It was shown in [30] and [25] that this reduced balance of the turbulent kinetic energy ceases to be valid near the edges of the turbulent shear layer. In terms of a slenderness parameter, those sublayers are very thin in comparison to the main layer. In the sublayers near the edges all four contributions to the turbulent kinetic energy balance, i.e. production by turbulent shear stresses, dissipation, diffusion and convection, are essential. The method of matched asymptotic expansions was applied in [31] to obtain solutions for plane, non-buoyant flows of mixing layers, jets and wakes, respectively. The same method could certainly be applied also to the present case of the buoyancy-controlled horizontal wake, but this is beyond the scope of the present work.

With regard to boundary conditions it is required that the turbulent kinetic energy vanishes at the wake edges, i.e.

$$\bar{h}(\zeta_B^\pm) = 0. \quad (82)$$

The vanishing of the turbulent kinetic energy at the wake edges has severe consequences with regard to the existence of the solutions. An inspection of the balance equation, Eq. (80) with (81), shows that the dimensionless turbulent kinetic energy vanishes proportional to $(\zeta - \zeta_B^\pm)^2$ as $\zeta \rightarrow \zeta_B^\pm$. This leads to a non-integrable singularity in the integral of Eq. (72) at the upper and lower bounds, i.e. $\zeta = \zeta_B^+$ and $\zeta = \zeta_B^-$, respectively. Obviously, it is a matter of modelling the apparent viscosity and, associated with it, the apparent thermal diffusivity according to Eqs. (81) and (54), respectively. Since those models are standard ones, we shall deal with the problem by replacing 0 on the right-hand side of Eq. (82) by a very small, positive constant; for details see the description of the numerical method in section 6.3.

With Eqs. (80) and (81) closure of the system of dimensionless basic equations, i.e. Eqs. (59), (60) and (70) for \bar{f} , \bar{g} and $\bar{\vartheta}$, is accomplished. The system of differential equations is of 7th order. It describes a boundary-value problem with two free boundaries, i.e. $\zeta = \zeta_B^+$ and $\zeta = \zeta_B^-$. To be satisfied are the boundary conditions Eqs. (58), (63) to (66), (68), (69) and (82), where all equations except Eqs. (58), (63) and (66) count for 2 boundary conditions each. But not all boundary conditions are independent conditions. First we note that the two smoothness conditions of Eq. (69) are satisfied if the transformed thermal energy equation, Eq. (70), with the boundary conditions of Eq. (64) are satisfied. Second, writing the right-hand side of the transformed momentum equation, Eq. (59), as $-(\bar{n}'\bar{f}'' + \bar{n}\bar{f}''')$, and inserting Eq. (81) for \bar{n} shows that the two smoothness conditions of Eq. (68) are also satisfied if, in addition to the momentum equation, the boundary conditions for the turbulent kinetic energy, i.e. Eq. (82),

are satisfied. In conclusion, the number of boundary conditions is in accord with the order of the system of differential equations supplemented by two independent free parameters.

6.3 Numerical solutions for the turbulent wake

For the purpose of obtaining numerical solutions it has turned out to be advantageous not to follow the straightforward procedure on the basis of the system of differential equations of 7th order as described in the last paragraph of the previous section. Instead, \bar{g} is eliminated from the system by inserting Eq. (60) into Eq. (59) and replacing the three boundary conditions, Eqs. (65) and (66), by the two conditions of Eq. (67). Thus, Eq. (60) is eliminated, and the order of the system is reduced to 6. The computation is then split into two steps. In the first step, the 6th order system of equations is solved for \bar{f} , $\bar{\vartheta}$, \bar{h} and the two independent free parameters ζ_B^+ and ζ_B^- . The right-hand side of Eq. (82) is replaced by 10^{-4} of the maximum value of \bar{h} to ensure the existence of the solution. In the second step, $\bar{g}(\zeta_B^-)$ is determined from Eq. (65) applied at ζ_B^- . The pressure profile $\bar{g}(\zeta)$ is then given by Eq. (62). As suggested by the formulation of the equations, the numerical solutions are performed with \tilde{Ri} as a parameter. For the presentation of the results, however, the use of Ri appears preferable, as it is defined in terms of basic parameters only.

The shooting method implemented in Wolfram Mathematica, which was employed for the computation of the laminar wake, did not lead to suitable solutions of the equations for the turbulent wake. Therefore, the system of equations was solved with the collocation solver “bvp4c” of MATLAB R2022a. This solver requires fixed prescribed positions of the boundaries. It was, however, observed that the same solution is obtained whenever the numerical boundaries are located outside of the actual wake. In such a case, the quantities \bar{f}' and \bar{h} become constant outside the wake. Therefore, the numerical boundaries were fixed at sufficient distance from the axis $\zeta = 0$. Placing the bottom and top boundaries at $\zeta = -0.3$ and $\zeta = 1.7$, respectively, was sufficient for all values of \tilde{Ri} . The locations of the wake edges ζ_B^+ and ζ_B^- were identified a posteriori as the positions where the temperature perturbation drops below 10^{-5} .

As an initial guess for $\bar{\vartheta}$ we have selected a cubic spline defined by the boundary conditions, Eqs. (58), (64) and (69). The initial guess for \bar{f}' was obtained as a stretched and shifted half-period of a sinus function, satisfying the boundary conditions, Eqs. (67) and (68). The initial guess for \bar{f} was then obtained by integration of \bar{f}' , using the boundary condition, Eq. (63). Finally, the initial guess for the turbulent kinetic energy was obtained by a mixing-length model as $\bar{h} \approx c_\mu c_l^2 (\bar{f}'')^2 / c_D$. The latter initial guess is only suitable for $\tilde{Ri} = O(1)$, as it implies the importance of the turbulent shear stress, which, however, turns out to be negligibly small for $\tilde{Ri} \ll 1$. To cope with that problem, solutions for $\tilde{Ri} \ll 1$ were obtained by numerical continuation.

A solution for $Ri = 0.25$ is shown in Fig. 4. The horizontal velocity component varies monotonously between the edge values. The vertical velocity component is negative on both sides of the wake, with the net entrainment into the wake being positive. Note that the vertical velocity component is very small, which a posteriori justifies the boundary-layer equations. Similar to the solution of the first kind for laminar flow, the temperature perturbation profile is wider at the upper side than at the lower side. However, in the turbulent case the asymmetry

of the $\tilde{\vartheta}$ -profile is much more pronounced. The reason for the asymmetry is the distribution of the turbulent kinetic energy \bar{h} and, as a consequence, of the turbulent thermal diffusivity. The turbulent kinetic energy is larger at the upper side of the wake, reaching a maximum at $\zeta = 0.197$, due to the buoyancy term $\tilde{\text{Ri}}\bar{f}\tilde{\vartheta}$ in the turbulent kinetic energy balance, Eq. (80). The buoyancy term acts as a source of turbulence for $\zeta > 0$ (unstable thermal stratification) and as a sink for $\zeta < 0$ (stable thermal stratification), as shown in Fig. 5. In the lower part of the wake, where the turbulent diffusivities are smaller, the profiles of the time-averaged flow quantities exhibit larger slopes and curvatures as compared to the upper part. Although Ri is by far not large in the case shown in Fig. 5, the production of turbulent kinetic energy is dominated by buoyancy in the upper part of the wake, while the contribution of the shear stress is comparatively small. The positive production by buoyancy in the upper part is compensated mainly by diffusion and dissipation. Diffusion transports turbulent kinetic energy towards the upper edge and into the lower part of the wake, where the contribution of buoyancy is negative. The lower part of the wake is dominated by the balance between the negative contribution of buoyancy and positive contribution of diffusion. The convection term is important near the upper edge, where its negative contribution compensates the positive diffusion and buoyancy terms.

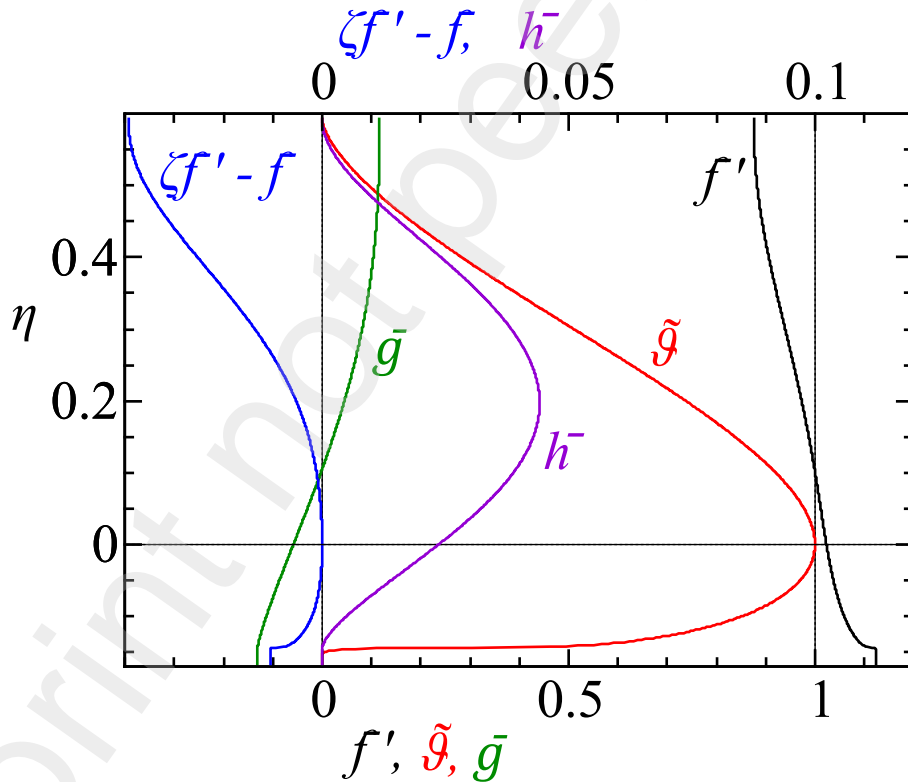


Fig. 4. Profiles of time-averaged flow quantities.
 $\text{Ri} = 0.25$, $C_\theta = 2.3$, $\zeta_B^- = -0.17$, $\zeta_B^+ = 0.59$

For values of Ri larger than about 2.1 solutions with reversed flow near the upper edge of the wake have been found. Furthermore, the numerical solutions lead to $\text{Ri} = 4.33$ as an upper bound for the existence of solutions. The latter result is in qualitative accord with the discussion of an upper bound for buoyancy as given in [28], p. 373. However, the

dimensionless lateral velocity component V , which is a measure of the slenderness of the shear layer, increases with increasing Richardson number. For $Ri = 1$ the magnitude of V is about 0.1. For substantially larger Richardson numbers the assumption of a slender shear layer is violated.

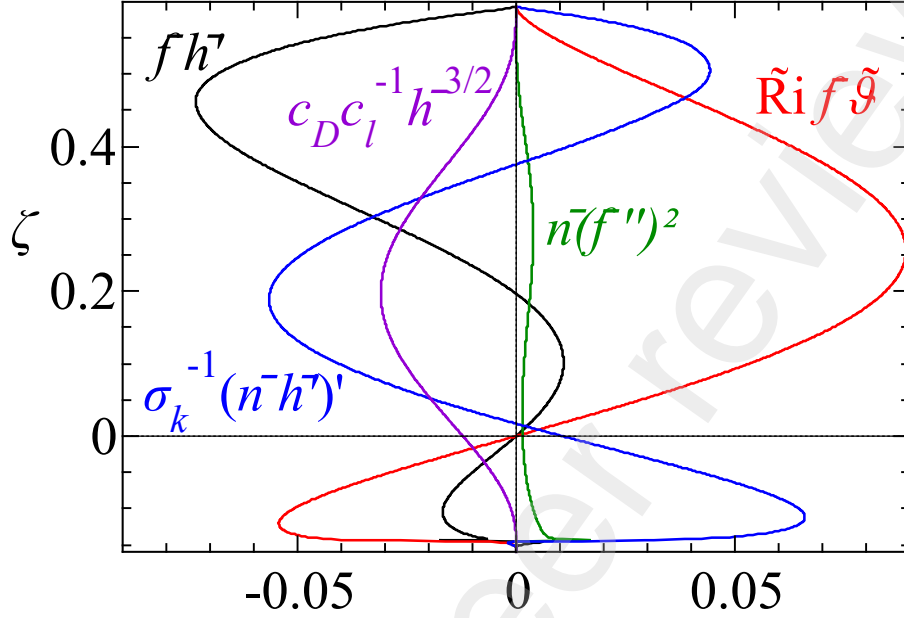


Fig. 5. Contributions to the balance of turbulent kinetic energy, Eq. (80).

$$Ri = 0.25, C_\theta = 2.3, \zeta_B^- = -0.17, \zeta_B^+ = 0.59.$$

$\bar{f}h'$...convection; $\bar{n}(\bar{f}'')^2$...production by shear stress; $\tilde{Ri}\bar{f}\tilde{\vartheta}$...production by buoyancy; $c_D c_l^{-1} \bar{h}^{3/2}$...dissipation; $\sigma_k^{-1}(\bar{n}h^7)'$...diffusion

6.4 Weak buoyancy effects

A parameter study with the numerical solutions revealed an interesting behavior of the turbulent wake properties for small values of Ri . Guided by the numerical results, the following power laws in terms of the effective Richardson number were found to be a proper description of the limit $\tilde{Ri} \rightarrow 0$:

$$\zeta = \tilde{Ri}^{1/3} z, \quad (83)$$

$$\bar{f} = \tilde{Ri}^{1/3} z + \tilde{Ri}^{5/3} F(z), \quad (84)$$

$$\bar{h} = \tilde{Ri}^{4/3} H(z), \quad (85)$$

$$\bar{n} = \tilde{Ri}^{2/3} N(z), \quad (86)$$

with z , F , H and N being quantities of the order 1. According to Eq. (83), the width of the wake vanishes proportional to $\tilde{Ri}^{1/3}$. As a normalized quantity, the temperature perturbation $\tilde{\vartheta}(\zeta) = \tilde{\vartheta}(\tilde{Ri}^{1/3} z)$ remains a quantity of the order 1, but the coefficient in Eq. (57) becomes

$$C_\theta = \tilde{Ri}^{-1/3} \tilde{C}_\theta, \quad \tilde{C}_\theta = O(1), \quad (87)$$

indicating that the temperature perturbation grows beyond bounds as $\tilde{Ri} \rightarrow 0$. This is in accord with the over-all thermal energy balance, cf. Section 4, as the width of the wake vanishes. With Eqs. (83) and (84), Eq. (71) gives in leading order

$$(\tilde{C}_\theta)^{-1} = \int_{z_B^-}^{z_B^+} \tilde{\vartheta}(\tilde{Ri}^{1/3}z) dz, \quad (88)$$

with $z_B^\pm = \tilde{Ri}^{-1/3} \zeta_B^\pm$ representing the z -values of the edges. Since the effective Richardson number is defined as $\tilde{Ri} = C_\theta Ri$, it follows from Eq. (87) that

$$Ri = (\tilde{C}_\theta)^{-1} \tilde{Ri}^{4/3} \quad (89)$$

in the limit $\tilde{Ri} \rightarrow 0$.

There is an interesting relationship between the velocity difference across the wake, i.e. $\Delta \bar{U} = \bar{f}'(\zeta_B^+) - \bar{f}'(\zeta_B^-)$, and the Richardson number. Taking $\bar{f}'(\zeta_B^+) - \bar{f}'(\zeta_B^-)$ from Eq. (67), transforming the variables from ζ to z by Eq. (83), and replacing the integral by $(\tilde{C}_\theta)^{-1}$ according to Eq. (88) shows that

$$\Delta \bar{U} = - Ri \quad \text{for } \tilde{Ri} \rightarrow 0. \quad (90)$$

This relationship is in accord with the analysis of the potential flow induced by both laminar and turbulent wake flows in the limit of weak buoyancy effects [12].

Introducing the asymptotic expansions Eqs. (83) to (86) into Eq. (59) gives the following momentum equation in leading order:

$$z(\ddot{F} + \tilde{\vartheta}) = - d(N\dot{F})/dz, \quad (91)$$

where dots refer to derivatives with respect to z . Similarly, the other basic equations and boundary conditions transform to equations that are free of \tilde{Ri} . Of particular interest is the balance equation for the turbulent kinetic energy. An inspection of Eq. (80) shows that the three terms representing convection, production due to buoyancy forces and diffusion of turbulent kinetic energy are all of the order of $\tilde{Ri}^{4/3}$, whereas the terms representing dissipation and the work done by the shear stress are of the order of \tilde{Ri}^2 and $\tilde{Ri}^{8/3}$, respectively, i.e. much smaller than the three first-mentioned terms. Thus, for $\tilde{Ri} \rightarrow 0$, Eq. (80) reduces to the following balance equation:

$$z(\dot{H} + \tilde{\vartheta}) + \sigma_k^{-1} d(N\dot{H})/dz = 0, \quad (92)$$

with

$$N = c_\mu c_l H^{1/2}. \quad (93)$$

Eq. (92) represents a balance of convection, production due to buoyancy forces and diffusion of turbulent kinetic energy. Dissipation is not required, as the production due to buoyancy forces is positive in a certain part of the wake, while it is negative in another part, with diffusion taking care of the necessary distribution.

The equations for the limit $\tilde{Ri} \rightarrow 0$ have been solved numerically by the same method as the full equations for $\tilde{Ri} = O(1)$, cf. Sections 6.2 and 6.3. The solution of the full equations for $\tilde{Ri} = 0.003$ is employed as an initial guess. Selected results are given in Figs. 6 to 8. To check the accuracy, the limiting profiles shown in Fig. 6 were compared with numerical solutions of

the full equations for the self-similar flow with the very small value $\tilde{Ri} = 0.003$ of the effective buoyancy parameter, and excellent agreement was found. Very good agreement is also found for the dependence of the flow quantities on the effective Richardson number, see Fig. 8. For the constants that appear in the limiting equations, the following values have been obtained: $\tilde{C}_\theta = 1.67$, $z_B^+ = 0.78$, $z_B^- = -0.33$.

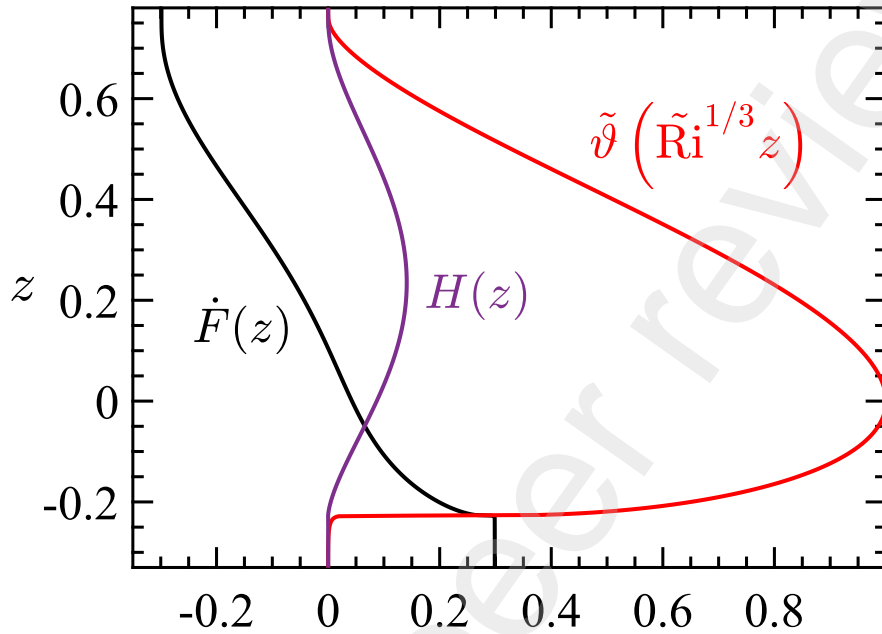


Fig. 6. Limiting profiles of longitudinal velocity perturbation, \dot{F} , turbulent kinetic energy, H , and normalized temperature perturbation, $\tilde{\vartheta}$.

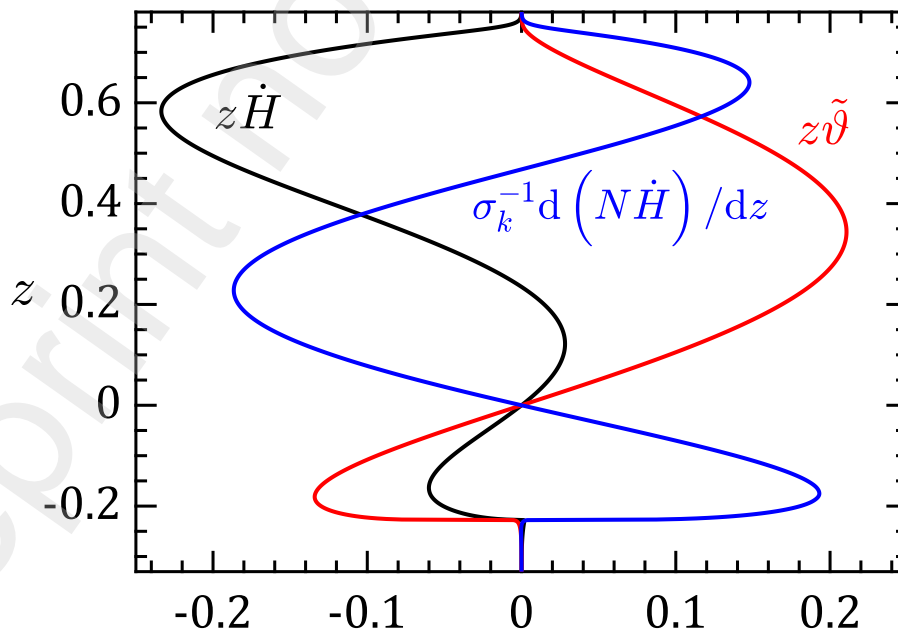


Fig. 7. Contributions to the balance of turbulent kinetic energy in the limit $\tilde{Ri} \rightarrow 0$, Eq. (92). $z\dot{H}$...convection; $z\tilde{\vartheta}$...production by buoyancy; $\sigma_k^{-1}d(N\dot{H})/dz$...diffusion

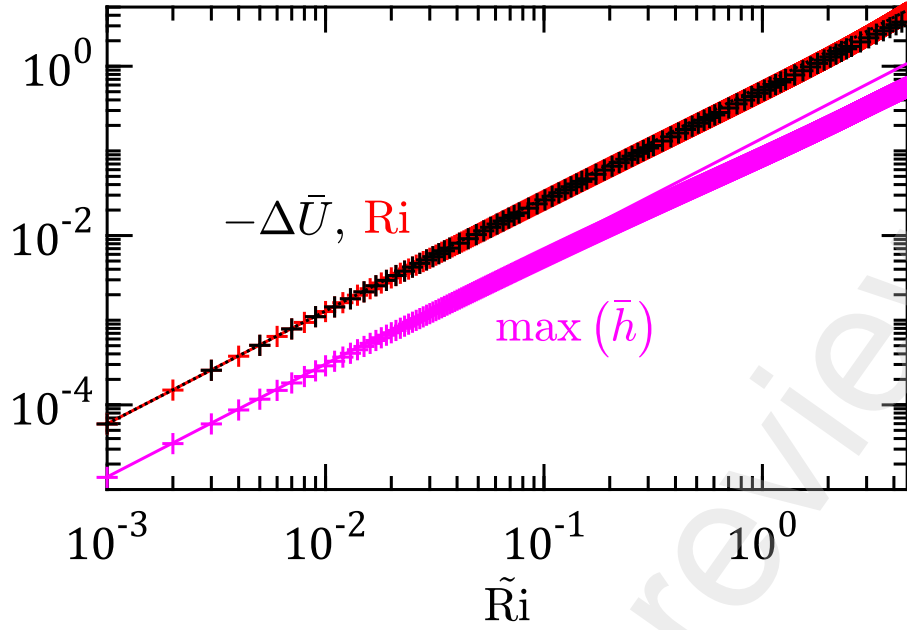


Fig. 8. Comparison of the asymptotic analysis with numerical solutions of the full equations for the self-similar turbulent wake flow: Ri , $\max(\bar{h})$, $\Delta\bar{U} = \bar{f}'(\zeta_B^+) - \bar{f}'(\zeta_B^-)$ vs. $\tilde{\text{Ri}}$.
Analysis: solid lines. Numerical results: +

The asymptotic behavior for $\tilde{\text{Ri}} \rightarrow 0$ according to Eq. (83) to (89) on the basis of Eqs. (47) to (52) is in contrast to the classical solution for the turbulent wake in the absence of buoyancy, i.e. for $\tilde{\text{Ri}} = 0$, cf. [6], pp. 655-659, 669-671. Written in terms of the present variables it is of the following form:

$$\bar{U} = 1 + \xi^{-1/2} f_0'(\eta), \quad (94)$$

$$\bar{\theta} = \xi^{-1/2} \vartheta_0(\eta), \quad (95)$$

with the similarity transformation

$$\xi = X; \quad \eta = Y/\sqrt{X}. \quad (96)$$

It is remarkable that this solution for the buoyancy-free wake, by contrast to the first-order solution for the buoyant wake with $\tilde{\text{Ri}} \rightarrow 0$, is associated with the drag coefficient of the body (plate) via an integral of $f_0'(\eta)$ over the wake cross-section, cf. [6], p. 669.⁷

For $\tilde{\text{Ri}} = 0$, Eqs. (94) and (95) show that the perturbation of the longitudinal velocity component as well as the temperature perturbation decay as $X^{-1/2}$ with increasing distance X from the plate. In case of $\tilde{\text{Ri}} \rightarrow 0$, however, it can be seen from Eqs. (55), (83) and (84) that the perturbation of the longitudinal velocity component, i.e. $\bar{f}' - 1$, is as small as $\tilde{\text{Ri}}^{4/3}$, but remains constant for $X \rightarrow \infty$. The opposite is true for the temperature perturbation, which is as large as $\tilde{\text{Ri}}^{-1/3}$, but decays as X^{-1} , i.e. more rapidly than in the case $\tilde{\text{Ri}} = 0$. Finally, the dimensionless width of the wake is proportional to $\tilde{\text{Ri}}^{1/3} X$ for $\tilde{\text{Ri}} \rightarrow 0$, whereas it is proportional to \sqrt{X} for $\tilde{\text{Ri}} = 0$, as can be seen from Eqs. (83) and (96), respectively. The

⁷ The differential equations and, consequently, the expressions given in [6] for the functions $f_0(\eta)$ and $\vartheta_0(\eta)$, respectively, are not applicable to the present analysis, as a different turbulence model is used.

obvious reason for those differences is the following. In the present analysis the basic equations are derived for $X \rightarrow \infty$ and then the limit $\tilde{Ri} \rightarrow 0$ is considered, whereas the case $\tilde{Ri} = 0$ corresponds to the opposite order of limits. To describe the transition from the solution for $\tilde{Ri} \rightarrow 0$ to the solution for $\tilde{Ri} = 0$ it is required to consider the double limit $\tilde{Ri} \rightarrow 0$ and $X \rightarrow \infty$. That analysis is beyond the scope of the present work.

7. Conclusions

The analysis presented above represents the leading order in an expansion for large distances from a horizontal plate, i.e. $X \rightarrow \infty$, where X is referred to the plate length. In this order the horizontal wake flow is affected only by the total heat flow from the plate, not by the drag force. The latter would only enter a second-order expansion.

The effects of buoyancy are characterized by a suitably defined Richardson number, Ri . The equations of motion together with the thermal energy equation reduce to boundary-layer equations, provided the shear layer is slender. This is the case if the Reynolds and Péclet numbers are very large and the Richardson number is of the order of 1 or smaller. Similarity transformations of the basic equations of both laminar and turbulent flows lead to sets of ordinary differential equations describing self-similar flows. The far-wake flow and the outer, potential flow are coupled, which is taken into account by matching conditions. In addition to the basic differential equations, the over-all thermal energy balance is of importance, as it governs the magnitude of the temperature perturbation. Remarkably, the power laws of the self-similar flows differ from the classical, i.e. non-buoyant, ones. A survey is given in the Table 1.

	m			
	laminar		turbulent	
	$Ri \neq 0$	$Ri = 0$	$Ri \neq 0$	$Ri = 0$
width of wake	1/2	1/2	1	1/2
longitudinal velocity perturbation	0	-1/2	0	-1/2
temperature perturbation	-1/2	-1/2	-1	-1/2

Table 1. Powers of distance from plate, X^m

Numerical solutions of the set of ordinary differential equations have revealed that there are two types of laminar far-wake flows, one of them featuring a region of reversed flow. Reversed flow cannot occur, however, at the boundaries of the laminar far wake. The existence of two types of far-wake flow, together with the possibility of reversed flow, indicates the usefulness of the far-wake solutions for the proper formulation of downstream boundary conditions in CFD applications, e.g. when the full Navier-Stokes equations are to be solved for the flow around a horizontal plate of finite length [4].

For turbulent flow, the balance of turbulent kinetic energy plays an important role. If the Richardson number is of the order of 1, the contributions of convection, production by the

Reynolds shear stress, dissipation, diffusion and production by gravity forces are all essential. For very small Richardson numbers, however, it turned out that production by gravity forces, though proportional to the Richardson number, outweighs dissipation and production by the Reynolds shear stress.

The numerical solutions are limited by upper bounds of the Richardson number. For laminar flow, the upper bound of the Richardson number is attained when the longitudinal velocity component vanishes at one of the wake boundaries, whereas in case of turbulent flow the upper bound of the Richardson number is attained when the stream function vanishes at one of the wake edges.

Since the wake width increases with increasing distance from the plate, the boundary-layer equations cease to be valid when the wake boundaries approach side walls of a horizontal channel. For details of this restriction see [12], Appendix D, and [13], Appendix B.

There is a possibility that buoyancy affects the boundary layer at a horizontal plate and induces an outer (potential) flow even if the over-all heat flow at the plate is zero. This can happen when one part of the plate is heated, while another part is cooled, leading to regions of positive and negative temperature perturbations in the wake. Numerical solutions of the full Navier-Stokes equations (to be published) revealed that in such a case the temperature perturbations decay faster than according to the self-similar flow solution. Consequently, a self-similar flow solution has not been found for $\dot{Q} = 0$.

Naturally, the present work reveals unsolved problems that deserve further investigations on horizontal wake flows with buoyancy. To be mentioned are, among others, the double limit of vanishing buoyancy and very large distance from the plate, or the stability of the horizontal laminar wake flow, associated with the transition to turbulent flow. Concerning desirable comparisons with measurements, it can be noted that unsteady buoyant horizontal wakes behind cylinders and other bluff bodies have been studied extensively [35–37]. Experimental investigations of buoyant horizontal wakes far behind horizontal plates or other streamlined objects that prevent vortex shedding are not known to the authors. However, the importance of buoyant production of turbulence in a horizontal turbulent boundary layer behind a heated wall-mounted obstacle has been demonstrated in [38].

Appendix A: Dissipation and work by pressure

a) Laminar flow

The thermal energy equation is supplemented by terms due to dissipation and work done by pressure, respectively. For laminar flow, the extended version of the energy equation in dimensionless form, i.e. Eq. (8), can then be written as

$$U \frac{\partial \theta}{\partial X} + V \frac{\partial \theta}{\partial Y} + T_{\infty} \beta_p N_d \text{Re} \left(U \frac{\partial P}{\partial X} + V \frac{\partial P}{\partial Y} \right) = \frac{1}{\text{Pe}} \frac{\partial^2 \theta}{\partial Y^2} + N_d \left(\frac{\partial U}{\partial Y} \right)^2, \quad (\text{A.1})$$

where the dimensionless parameter N_d , defined as

$$N_d = \nu \rho_{\infty} u_{\infty}^2 / \dot{Q}, \quad (\text{A.2})$$

characterizes the effect of dissipation in the present problem. Since the energy equation is not homogeneous anymore, we refrain here from normalizing the temperature perturbation as it is

done in the main part of the paper. Introducing, again, the boundary-layer stretching according to Eqs. (19) and (20), Eq. (A.1) becomes:

$$\Psi_{\hat{Y}}\theta_X - \Psi_X\theta_{\hat{Y}} + T_{\infty}\beta_p N_d \text{Re}(\Psi_{\hat{Y}}P_X - \Psi_X P_{\hat{Y}}) = \text{Pr}^{-1}\theta_{\hat{Y}\hat{Y}} + N_d \text{Re}(\Psi_{\hat{Y}\hat{Y}})^2. \quad (\text{A.3})$$

This is the extended version of Eq. (23). In accord with the Boussinesq approximation, the isobaric expansivity, β_p , has been assumed constant. We take the free-stream absolute temperature, T_{∞} , as the reference temperature for β_p . It is then consistent that T has been replaced by T_{∞} in the coefficient of the pressure-work term in Eq. (A.1).

Next, the similarity transformation according to Eqs. (24) to (27) is applied. We obtain

$$2\vartheta'' + \text{Pr}(f\vartheta)' = -N_d \text{Pe}\sqrt{\xi}[2(f'')^2 + T_{\infty}\beta_p f g']. \quad (\text{A.4})$$

Eq. (A.4) is an extended version of Eq. (34). The extension consists of the two terms on the right-hand side of Eq. (A.4), with the first term representing dissipation, while the second term is due to the work done by the pressure. Obviously, Eq. (A.4) is not in accord with the assumed self-similarity, but it may serve to provide conditions for neglecting dissipation and pressure work. If $T_{\infty}\beta_p \ll 1$, as it is the case for common liquids, the effect of the pressure work is much smaller than the effect of dissipation. For common gases, however, $T_{\infty}\beta_p = O(1)$, with $T_{\infty}\beta_p = 1$ for the special case of perfect gases. The work done by the pressure is then of the same order of magnitude as dissipation. With regard to the latter, Eq. (A.4) shows that it increases with increasing distance from the plate. However, N_d is, in general, very small. In order to estimate the order of magnitude, it is convenient to relate \dot{Q} to a characteristic temperature difference between the plate surface and the free-stream temperature, i.e. $(T_w - T_{\infty})$. Introducing the Stanton number

$$\text{St} = \dot{Q}/\rho_{\infty}u_{\infty}Lc_p(T_w - T_{\infty}), \quad (\text{A.5})$$

we obtain

$$N_d = \text{Ec}/\text{StRe}, \quad (\text{A.6})$$

where Ec is the Eckert number, i.e.

$$\text{Ec} = u_{\infty}^2/c_p(T_w - T_{\infty}). \quad (\text{A.7})$$

According to the present definitions both N_d and Ec are positive for a heated plate, whereas they are negative in case of a cooled plate. From the theory of mixed convection flow over horizontal plates, cf. [27], it is known that $\text{St}\sqrt{\text{Re}} = O(1)$, depending somewhat on the Prandtl number. Thus, discarding the influence of the Prandtl number, the coefficient on the right-hand side of Eq. (A.4) is of the following order of magnitude:

$$|N_d|\text{Pe}\sqrt{\xi} = O(|\text{Ec}|\sqrt{\text{Re}_{\xi}}), \quad (\text{A.8})$$

where $\text{Re}_{\xi} = \text{Re}\xi$ is the Reynolds number in terms of the distance from the plate. It follows from Eq. (A.4) that dissipation is negligible in the energy equation if $|\text{Ec}|\sqrt{\text{Re}_{\xi}} \ll 1$. For water, for instance, with $u_{\infty} = 1$ m/s and $|T_w - T_{\infty}| = 25$ K, $|\text{Ec}|$ is about 10^{-5} . This value is so small that dissipation would become of importance at values of Re_{ξ} that are so extremely large that transition from laminar to turbulent flow has certainly already taken place.

b) Turbulent flow

If the thermal energy equation (A.1) is written in terms of ensemble-averaged variables, the last term on the right-hand side is due to direct dissipation. In addition, there is a contribution of the turbulent dissipation to the thermal energy equation, see [6], p. 510. By suitably combining the contributions of viscous diffusion and turbulent dissipation, cf. [6], pp. 508 and 509, the turbulent dissipation rate is equal to the quantity ε that appears in the balance of turbulent kinetic energy, Eq. (74). Using Eqs. (76), (77) and (79) to express ε in terms of the dimensionless turbulent kinetic energy \bar{h} , the thermal energy equation for the turbulent wake becomes

$$\bar{U}\frac{\partial\bar{\theta}}{\partial X} + \bar{V}\frac{\partial\bar{\theta}}{\partial Y} + T_\infty\beta_p N_d \text{Re} \left(\bar{U}\frac{\partial\bar{P}}{\partial X} + \bar{V}\frac{\partial\bar{P}}{\partial Y} \right) = \frac{\partial}{\partial Y} \left(\frac{1}{\text{Pe}_t} \frac{\partial\bar{\theta}}{\partial Y} \right) + N_d \left(\frac{\partial\bar{U}}{\partial Y} \right)^2 + \frac{c_D N_d \text{Re}}{c_l C_B X} \bar{h}^{3/2}, \quad (\text{A.9})$$

where the dissipation parameter N_d has been introduced according to Eq. (A.2). Normalizing the temperature perturbation according to Eq. (57) and applying then the similarity transformation according to Sections 6.1 and 6.2, we obtain:

$$(\bar{f}\tilde{\vartheta})' + (\bar{a}\tilde{\vartheta}')' = - (N_d/C_\theta) \{ (\bar{f}'')^2 + \text{Re} [T_\infty\beta_p \bar{f}\bar{g}' + c_D C_B^{-1} c_l^{-1} \bar{h}^{3/2}] \xi \}. \quad (\text{A.10})$$

The terms due to direct dissipation, pressure work and turbulent dissipation, in this order, are given on the right-hand side of Eq. (A.10).

The orders of magnitude are now estimated for substantial buoyancy effects, i.e. $\tilde{\text{Ri}} = O(1)$, as follows. First we note that the empirical constant c_D is of the order of 1, $(1/C_\theta)$ is of the order of the slenderness parameter C_B , which is of the order of 1 for $\tilde{\text{Ri}} = O(1)$. Secondly, we repeat that $T_\infty\beta_p$ is of the order 1 or even much smaller. Thus the term due to the work done by the pressure is, at most, of the same order of magnitude as the turbulent dissipation term. It remains to estimate the magnitude of N_d . Since it is just a matter of definitions, Eq. (A.6) can be applied. Assuming that the flow is laminar at the plate and the transition to turbulent flow takes place in the wake, which will be rather the rule than the exception, cf. [39], the estimate $\text{St}\sqrt{\text{Re}} = O(1)$ remains valid. It follows that

$$|N_d| = O(|\text{Ec}|/\sqrt{\text{Re}}). \quad (\text{A.11})$$

Since the Eckert number is characteristically extremely small, as discussed above, and, furthermore, the Reynolds number is assumed to be very large for the present analysis, the term due to direct dissipation, i.e. $(N_d/C_\theta)(\bar{f}'')^2$, is certainly negligible in Eq. (A.10). The term due to turbulent dissipation, however, is seen to be proportional to ξ , i.e. the dimensionless distance from the plate. Thus, it grows beyond bounds as $\xi \rightarrow \infty$. However, the distance where the turbulent-dissipation term becomes of the same order of magnitude as the leading terms in Eq. (A.10) is so large that it will hardly be of relevance to applications. Besides, there are also other reasons for a possible break-down of the boundary-layer equations, as briefly discussed in the Conclusions.

It remains to be noted that in the limit of very weak buoyancy effects, i.e. $\tilde{\text{Ri}} \rightarrow 0$, the slenderness parameter C_B is as small as $\tilde{\text{Ri}}^{1/3}$, cf. Eq. (83). The slope of the velocity profile is even smaller, i.e. $\bar{f}'' = O(\tilde{\text{Ri}})$. Since $1/C_\theta = O(\tilde{\text{Ri}}^{1/3})$ according to Eq. (87), $(N_d/C_\theta)(\bar{f}'')^2$ is as small as $N_d \tilde{\text{Ri}}^{7/3}$, and neglecting that term in the thermal energy equation is even more

justified in the limiting case than in the general case of $\tilde{R}i = O(1)$. Estimates of the other terms on the right-hand side of Eq. (A.10) lead to similar conclusions.

Appendix B: Asymptotic behavior of the solutions for laminar flow as $\eta \rightarrow \pm \infty$

It may be of general interest and, furthermore, be useful for the numerical solution, to know the asymptotic behavior of the dependent variables near the boundaries of the wake. For that purpose we insert the following relationships into the system of equations given in Section 5.3 and consider the limit $\eta \rightarrow \pm \infty$:

$$f = F_1^\pm \eta + F_2^\pm + \varphi^\pm(\eta), \quad (\text{B.1})$$

$$g = G^\pm + \gamma^\pm(\eta), \quad (\text{B.2})$$

$$\tilde{\vartheta} = \vartheta^\pm(\eta), \quad (\text{B.3})$$

with $(F_{1,2}^\pm, G^\pm) = \text{const} = O(1)$ and $(\varphi^\pm, \gamma^\pm, \vartheta^\pm) \rightarrow 0$ as $\eta \rightarrow \pm \infty$. From Eq. (41) one obtains

$$\vartheta^\pm = \exp\left(-\frac{\text{Pr}}{4} F_1^\pm \eta^2\right). \quad (\text{B.4})$$

This result shows that the boundary condition Eq. (37) requires positive values of F_1^\pm , i.e.

$$F_1^\pm > 0. \quad (\text{B.5})$$

Since $U = f'$ according to Eq. (28), Eq. (B.5) indicates that there is no reversed flow at the wake boundaries.

The matching condition Eq. (38) shows that the constants have to satisfy the relation

$$F_1^\pm = (1 - 2G^\pm)^{1/2}. \quad (\text{B.6})$$

This equation requires that

$$G^\pm < 1/2. \quad (\text{B.7})$$

In view of Eq. (B.2), Eq. (B.7) expresses a bound for the pressure perturbation that has to be obeyed by the solution of the differential equations.

The result for the temperature disturbance, Eq. (B.4), can be inserted into Eqs. (33) and (32) to obtain the following relations for the pressure and velocity disturbances, respectively:

$$(\gamma^\pm)' = \tilde{K} \exp\left(-\frac{\text{Pr}}{4} F_1^\pm \eta^2\right), \quad (\text{B.8})$$

$$2(\varphi^\pm)''' + F_1^\pm \eta (\varphi^\pm)'' + \tilde{K} \eta \exp\left(-\frac{\text{Pr}}{4} F_1^\pm \eta^2\right) = 0. \quad (\text{B.9})$$

Eq. (B.8) can be integrated to obtain

$$\gamma^\pm = -\left(2\tilde{K}/\text{Pr}F_1^\pm\eta\right) \exp\left(-\frac{\text{Pr}}{4} F_1^\pm \eta^2\right). \quad (\text{B.10})$$

Eq. (B.9) is a linear, inhomogeneous differential equation of first order for $(\varphi^\pm)''$. The general solution of the homogeneous part is discarded, as it represents a solution of the problem of vanishing buoyancy, which is of no interest here. What remains is the following particular solution of the inhomogeneous Eq. (B.9):

$$(\varphi^\pm)'' = [\tilde{K}/(\text{Pr} - 1)F_1^\pm] \exp\left(-\frac{\text{Pr}}{4}F_1^\pm\eta^2\right) \text{ for } \text{Pr} \neq 1, \quad (\text{B.11})$$

$$(\varphi^\pm)'' = -\frac{1}{4}\tilde{K}\eta^2 \exp\left(-\frac{1}{4}F_1^\pm\eta^2\right) \text{ for } \text{Pr} = 1. \quad (\text{B.12})$$

The coefficient on the right-hand-side of Eq. (B.11) grows beyond bounds as $\text{Pr} \rightarrow 1$. Thus the case $\text{Pr} = 1$ has resonance properties.

The decay of the velocity component U to its limiting value at the boundary of the wake is represented by $(\varphi^\pm)'$, which can be obtained by integrating Eqs. (B.11) and (B.12). The first integral can be expressed in terms of the complimentary error function, whereas integrating Eq. (B.12) would have to be done numerically.

The results indicate a very strong exponential decay of all perturbations as $\eta \rightarrow \pm \infty$, as it is also the case for classical boundary layers, cf. [40], p. 226.

A quantity of particular interest is the lateral velocity for $\eta \rightarrow \pm \infty$, as it represents the entrainment of mass into the wake. From Eqs. (29) and (B.1) one obtains

$$\hat{V} = -(1/2)\xi^{-1/2}F_2^\pm, \quad (\text{B.13})$$

i.e., the constant F_2^\pm , as introduced in Eq. (B.1), gives the entrainment.

As is natural for asymptotic expansions, the constants G^\pm (or F_1^\pm) and F_2^\pm remain free and are to be determined in course of numerical solutions of the differential equations.

Acknowledgements

The authors gratefully acknowledge the financial support by Androsch International Consulting GmbH, Vienna, for enabling this research. This funding source was neither involved in choosing the topic of research nor in the decision to submit the article for publication.

References

- [1] G.E. Robertson, J.H. Seinfeld, L.G. Leal, Combined forced and free convection flow past a horizontal flat plate, *AICHE J.* 19 (1973) 998–1008. <https://doi.org/10.1002/aic.690190517>.
- [2] V. Noshadi, W. Schneider, A numerical investigation of mixed convection on a horizontal semi-infinite plate, in: H.J. Rath, C. Egbers (Eds.), *Advances in Fluid Mechanics and Turbomachinery*, Springer-Berlin, 1998: pp. 87–97. https://doi.org/10.1007/978-3-642-72157-1_8.
- [3] L. Bátor, Numerical investigation of mixed convection flow over a heated horizontal plate of finite length, *PAMM* 23 (2023) e202300030. <https://doi.org/10.1002/pamm.202300030>.
- [4] L. Bátor, W. Schneider, E. Bozsó, Mixed convection flow over a horizontal plate and the horizontal wake far downstream, in: *Proc. 9th Plenary Eurotherm Conf.*, Bled, Slovenia, 2024. <https://doi.org/10.1088/1742-6596/2766/1/012061>.

- [5] J. Denier, P.W. Duck, J. Li, On the growth (and suppression) of very short-scale disturbances in mixed forced–free convection boundary layers, *J. Fluid Mech.* 526 (2005) 147–170. <https://doi.org/10.1017/S0022112004002782>.
- [6] H. Schlichting, K. Gersten, *Boundary-Layer Theory*, 9th ed., Springer-Verlag Berlin, Heidelberg, 2017. <https://doi.org/10.1007/978-3-662-52919-5>.
- [7] P. Ehrhard, Laminar mixed convection in two-dimensional far wakes above heated/cooled bodies: model and experiments, *J. Fluid Mech.* 439 (2001) 165–198. <https://doi.org/10.1017/S0022112001004463>.
- [8] H. Steinrück, Mixed convection over a horizontal plate: self-similar and connecting boundary-layer flows, *Fluid Dyn. Res.* 15 (1995) 113–127. [https://doi.org/10.1016/0169-5983\(94\)00052-2](https://doi.org/10.1016/0169-5983(94)00052-2).
- [9] V. Noshadi, W. Schneider, Horizontal jets due to natural convection, *ZAMM* 75 (1995) S1 351-352.
- [10] V. Noshadi, W. Schneider, Natural convection flow far from a horizontal plate, *J. Fluid Mech.* 387 (1999) 227–254. <https://doi.org/10.1017/S0022112099004462>.
- [11] W. Schneider, Mixed convection at a finite horizontal plate, in: E.W.P. Hahne, W. Heidemann, K. Spindler (Eds.), *Proc. 3rd European Thermal Sci. Conf.*, Edizione ETS, Pisa, 2000: pp. 195–198.
- [12] W. Schneider, Lift, thrust and heat transfer due to mixed convection flow past a horizontal plate of finite length, *J. Fluid Mech.* 529 (2005) 51–69. <https://doi.org/10.1017/S0022112004002940>.
- [13] M. Müllner, W. Schneider, Laminar mixed convection on a horizontal plate of finite length in a channel of finite width, *Heat Mass Transfer* 46 (2010) 1097–1110. <https://doi.org/10.1007/s00231-010-0679-2>.
- [14] H. Steinrück, Lj. Savić, The trailing edge problem for mixed convection flow past a horizontal plate, in: W. Gutkowski, T.A. Kowalewski (Eds.), *Proc. 21st Intl. Congr. Theor. Appl. Mech.*, IPPT PAN, Warszawa, 2004: p. FM2 12030.
- [15] Lj. Savić, H. Steinrück, The trailing-edge problem for mixed-convection flow past a horizontal plate, *J. Fluid Mech.* 588 (2007) 309–330. <https://doi.org/10.1017/S0022112007007744>.
- [16] Lj. Savić, H. Steinrück, Mixed convection flow past a horizontal plate, in: *Proc. 25th Yugoslav Congr. Theor. Appl. Mech.*, Novi Sad, 2005. <https://doi.org/10.2298/TAM0501001S>.
- [17] H. Steinrück, B. Kotesovec, A thermally induced singularity in a wake, in: A.F. Hegarty, N. Kopteva, E. O’ Riordan, M. Stynes (Eds.), *Proc. BAIL 2008 – Boundary and Interior Layers*, Limerick, Ireland, Springer, 2009: pp. 237–246. https://doi.org/10.1007/978-3-642-00605-0_19.
- [18] H. Steinrück, Interaction mechanisms in the mixed convection flow past a horizontal plate, in: H. Steinrück (Ed.), *Asymptotic Methods in Fluid Mechanics: Survey and Recent Advances*, CISM Courses and Lectures, Springer, Wien New York, 2010: pp. 287–310. https://doi.org/10.1007/978-3-7091-0408-8_9.

- [19] H. Steinrück, The mixed convection flow past a horizontal plate in a channel: wake-potential flow interaction, in: PAMM-Proc. Appl. Math. Mech., 2011: pp. 591–592. <https://doi.org/10.1002/pamm.201110285>.
- [20] S. Julien, S. Oritz, J.-M. Chomaz, Secondary instability mechanisms in the wake of a flat plate, *Eur. J. Mech. B/Fluids* 23 (2004) 157–165. <https://doi.org/10.1016/j.euromechflu.2003.07.001>.
- [21] M.J. Taylor, N. Peake, A note on the absolute instability of wakes, *Eur. J. Mech. B/Fluids* 18 (1999) 573–579. [https://doi.org/10.1016/S0997-7546\(99\)00108-9](https://doi.org/10.1016/S0997-7546(99)00108-9).
- [22] H. Herwig, K. Gersten, *Strömungsmechanik*, Vieweg-Verlag, Braunschweig/Wiesbaden, 1992.
- [23] H. Herwig, S.P. Mahulikar, Variable property effects in single-phase incompressible flows through microchannels, *Int. J. Thermal Sci.* 45 (2006) 977–981. <https://doi.org/10.1016/j.ijthermalsci.2006.01.002>.
- [24] S.P. Mahulikar, H. Herwig, Physical effects in laminar microconvection due to variations in incompressible fluid properties, *Phys. Fluids* 18 (2006) 073601. <https://doi.org/10.1063/1.2210027>.
- [25] W. Schneider, Boundary-layer theory of free turbulent shear flows, *Z. Flugwiss. Weltraumforsch. (ZFW)* 15 (1991) 143–158.
- [26] H. Herwig, An asymptotic approach to free-convection flow at maximum density, *Chem. Eng. Sci.* 40 (1985) 1709–1715. [https://doi.org/10.1016/0009-2509\(85\)80032-4](https://doi.org/10.1016/0009-2509(85)80032-4).
- [27] W. Schneider, A similarity solution for combined forced and free convection flow over a horizontal plate, *Int. J. Heat Mass Transfer* 22 (1979) 1401–1406. [https://doi.org/10.1016/0017-9310\(79\)90202-3](https://doi.org/10.1016/0017-9310(79)90202-3).
- [28] A.A. Townsend, *The Structure of Turbulent Shear Flow*, 2nd ed., Cambridge University Press, Cambridge, 1976.
- [29] W. Rodi, *Turbulence Models and their Application in Hydraulics*, 3rd ed., A.A.Balkema, Rotterdam, 1993. <https://doi.org/10.1201/9780203734896>.
- [30] W. Schneider, K. Mörwald, Asymptotic analysis of turbulent free shear layers, in: *Proc. Beijing Intl. Conf. Fluid Mech.*, Peking Univ. Press, Beijing, 1988: pp. 50–55. <https://doi.org/10.1016/B978-0-08-036232-8.50014-1>.
- [31] K. Mörwald, *Asymptotische Theorie freier turbulenter Scherströmungen*, Doctoral thesis, TU Wien, 1988.
- [32] K. Mörwald, W. Schneider, Asymptotic structure of turbulent free shear layers and implications for turbulence modelling, *ZAMM-Z. Angew. Math. Mech.* 69 (1989) T626–T627. <https://doi.org/10.1002/zamm.19890690603>.
- [33] J.C. Rotta, *Turbulente Strömungen*, Verlag B.G. Teubner, Stuttgart, 1972. <https://doi.org/10.1007/978-3-322-91206-0>.
- [34] H. Tennekes, J.L. Lumley, *A First Course in Turbulence*, MIT Press, Cambridge, 1972.

- [35] R.N. Kieft, C.C.M. Rindt, A.A. van Steenhoven, The wake behaviour behind a heated horizontal cylinder, *Exp. Therm. Fluid Sci.* 19 (1999) 183–193. [https://doi.org/10.1016/S0894-1777\(99\)00021-7](https://doi.org/10.1016/S0894-1777(99)00021-7).
- [36] R.N. Kieft, C.C.M. Rindt, A.A. van Steenhoven, G.J.F. van Heijst, On the wake structure behind a heated horizontal cylinder in cross-flow, *J. Fluid Mech.* 486 (2003) 189–211. <https://doi.org/10.1017/S0022112003004567>.
- [37] A.A. van Steenhoven, C.C.M. Rindt, Flow transition behind a heated cylinder, *Int. J. Heat Fluid Flow* 24 (2003) 322–333. [https://doi.org/10.1016/S0142-727X\(03\)00023-7](https://doi.org/10.1016/S0142-727X(03)00023-7).
- [38] Y.S. Mori, K. Hishida, M. Maeda, Buoyancy effects on the wake behind a heated obstacle immersed in a turbulent boundary layer, *Int. J. Heat Fluid Flow* 16 (1995) 405–416. [https://doi.org/10.1016/0142-727X\(95\)00055-U](https://doi.org/10.1016/0142-727X(95)00055-U).
- [39] K. Venkatasubbaiah, The effect of buoyancy on the stability mixed convection flow over a horizontal plate, *Eur. J. Mech. B/Fluids* 30 (2011) 526–533. <https://doi.org/10.1016/j.euromechflu.2011.05.002>.
- [40] C.W. Jones, E.J. Watson, Two-dimensional boundary layers, in: L. Rosenhead (Ed.), *Laminar Boundary Layers*, Clarendon Press, Oxford, 1963.

Captions of figures

Fig. 1. The horizontal wake flow far downstream of a horizontal plate with temperature and pressure profiles (schematic).

Fig. 2. A solution of the first kind: Profiles of horizontal velocity component f' (black), normalized temperature perturbation $\tilde{\vartheta}$ (red), pressure perturbation g (green) and vertical velocity component $\eta f' - f$ (blue). $\tilde{K} = 1/4$, $Pr = 1$.

Fig. 3. A solution of the second kind: Profiles of flow quantities, distinguished by color. $\tilde{K} = 0.04$, $Pr = 1$.

Fig. 4. Profiles of time-averaged flow quantities.

$Ri = 0.25$, $C_\theta = 2.3$, $\zeta_B^- = -0.17$, $\zeta_B^+ = 0.59$

Fig. 5. Contributions to the balance of turbulent kinetic energy, Eq. (80).

$Ri = 0.25$, $C_\theta = 2.3$, $\zeta_B^- = -0.17$, $\zeta_B^+ = 0.59$.

$\overline{f'h'}$...convection; $\overline{n}(\overline{f''})^2$...production by shear stress; $\tilde{Ri}\tilde{f}\tilde{\vartheta}$...production by buoyancy; $c_D c_l^{-1} \overline{h}^{3/2}$...dissipation; $\sigma_k^{-1}(\overline{nh'})'$...diffusion

Fig. 6. Limiting profiles of longitudinal velocity perturbation, \tilde{F} , turbulent kinetic energy, H , and normalized temperature perturbation, $\tilde{\vartheta}$.

Fig. 7. Contributions to the balance of turbulent kinetic energy in the limit $\tilde{Ri} \rightarrow 0$, Eq. (92). $z\dot{H}$...convection; $z\tilde{\vartheta}$...production by buoyancy; $\sigma_k^{-1}d(N\dot{H})/dz$...diffusion

Fig. 8. Comparison of the asymptotic analysis with numerical solutions of the full equations for the self-similar turbulent wake flow: Ri , $\max(\overline{h})$, $\Delta\overline{U} = \overline{f}'(\zeta_B^+) - \overline{f}'(\zeta_B^-)$ vs. \tilde{Ri} .

Analysis: solid lines. Numerical results: +